International Geology Review

ISSN: 0020-6814 (Print) 1938-2839 (Online) Journal homepage: http://www.tandfonline.com/loi/tigr20

Legacy of the California Gold Rush: Environmental Geochemistry of Arsenic in the Southern Mother Lode Gold District

Kaye S. Savage , Dennis K. Bird & Roger P. Ashley

To cite this article: Kaye S. Savage , Dennis K. Bird & Roger P. Ashley (2000) Legacy of the California Gold Rush: Environmental Geochemistry of Arsenic in the Southern Mother Lode Gold District, International Geology Review, 42:5, 385-415, DOI: 10.1080/00206810009465089

To link to this article: https://doi.org/10.1080/00206810009465089

International Geology Review, Vol. 42, 2000, p. 385–415.

Legacy of the California Gold Rush: Environmental Geochemistry of Arsenic in the Southern Mother Lode Gold District

KAYE S. SAVAGE, DENNIS K. BIRD,

Department of Geological and Environmental Sciences, Stanford University, Stanford, California 94305

AND ROGER P. ASHLEY

U.S. Geological Survey, Menlo Park, California, 94025

Abstract

Gold mining activity in the Sierra Nevada foothills, both recently and during the California Gold Rush, has exposed arsenic-rich pyritic rocks to weathering and erosion. This study describes arsenic concentration and speciation in three hydrogeologic settings in the southern Mother Lode Gold District: mineralized outcrops and mine waste rock (overburden); mill tailings submerged in a water reservoir; and lake waters in this monomictic reservoir and in a monomictic lake developing within a recent open-pit mine. These environments are characterized by distinct modes of rock-water interaction that influence the local transport and fate of arsenic. Arsenic in outcrops and waste rock occurs in arsenian pyrite containing an average of 2 wt% arsenic. Arsenic is concentrated up to 1300 ppm in fine-grained, friable, iron-rich weathering products of the arsenian pyrite (goethite, jarosite, copiapite), which develop as efflorescences and crusts on weathering outcrops. Arsenic is sorbed as a bidentate complex on goethite, and substitutes for sulfate in jarosite.

Submerged mill tailings obtained by gravity core at Don Pedro Reservoir contain arsenic up to 300 ppm in coarse sand layers. Overlying surface muds have less arsenic in the solid fraction but higher concentrations in porewaters (up to 500 μg/L) than the sands. Fine quartz tailings also contain up to 3.5 ppm mercury related to the ore processing. The pH values in sediment porewaters range from 3.7 in buried gypsum-bearing sands and tailings to 7 in the overlying lake sediments. Reservoir waters immediately above the cores contain up to 3.5 μg/L arsenic; lake waters away from the submerged tailings typically contain less than 1 μg/L arsenic.

Dewatering during excavation of the Harvard open-pit mine produced a hydrologic cone of depression that has been recovering toward the pre-mining groundwater configuration since mining ended in 1994. Aqueous arsenic concentrations in the 80 m deep pit lake are up to 1000 μg/L. Redistribution of the arsenic occurs during summer stratification, with highest concentrations at middle depths. The total mass of arsenic in the pit lake increases coinciding with early winter rains that erode, partially dissolve, and transport arsenic-bearing salts into the pit lake.

Arsenic concentration, speciation, and distribution in the Sierra Nevada foothills depend on many factors, including the lithologic sources of arsenic, climatic influences on weathering of host minerals, and geochemical characteristics of waters with which source and secondary minerals react. Oxidation of arsenian pyrite to goethite, jarosite, and copiapite causes temporary attenuation of arsenic during summer, when these secondary minerals accumulate; subsequent rapid dissemination of arsenic into the aqueous environment is caused by annual winter storms. As the population of the Mother Lode area grows, it is increasingly important to consider these effects during planning and development of land and groundwater resources.

Introduction

THE CALIFORNIA GOLD RUSH of the mid-nineteenth century had far-reaching impacts on the economy and landscape of the western United States. Many changes were evident even in the early years, including diverse populations of settlers, development of major cities and numerous small towns, and resculpting of mountains, rivers, and streams by hard-rock and hydraulic miners in the Sierra Nevada foothills. However, the effects of environmental contaminants such as arsenic and mercury have only come to light recently as the Sierra Nevada foothills region experiences a new population boom spurred on by relatively inexpensive and

0020-6814/00/456/385-31 $10.00

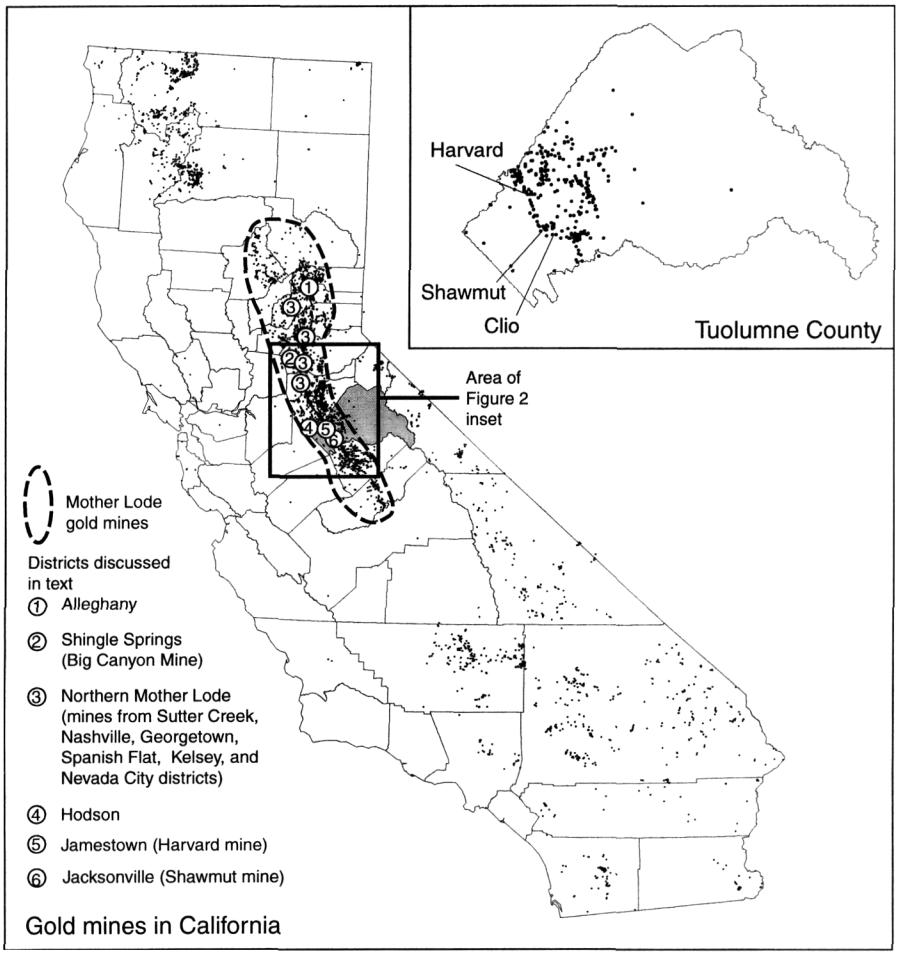

FIG. 1. Locations of gold mines in California; county boundaries are shown for reference (U.S. Geological Survey Computer Resources Information Bank). Mother Lode gold mines are enclosed by the dashed line. Circled numbers represent districts for which analyses are presented. Tuolumne County is shaded. Inset shows locations of gold mines included in this study; Tuolumne County boundary and additional mines shown for reference.

available land, the natural beauty of the area, historic attractions, and a strong tourist industry. The increased demands for land and water supplies in the gold-mining region have increased the need for a clear understanding of the potential risks associated with developing former mine lands, such as contaminated water and soils.

Arsenic concentrated at the Earth's surface by mining activities in the Mother Lode Gold District (Fig. 1) has already raised concerns at several sites. Extensive remediation was conducted in the mid-1990s at the Mesa D'Oro subdivision of Sutter Creek (Fig. 2, inset), where homes were constructed on tailings of the Central Eureka mine (Ziarkowski, 1999). Another site in the northern Mother Lode was recently declared a Superfund site after a dam failure released fine-grained, arsenic-rich mill tailings from the Lava Cap mine into Little Clipper Creek and Lost Lake, a small recreational pond (Ashley and Ziarkowski, 1999). One site addressed in this study, the Jamestown mine, is presently of concern to the Central Valley Regional Water Quality Control Board because of high arsenic concentrations and total dissolved solids in ground and surface waters (Central Valley Regional Water Quality Control Board meeting, Sept. 17, 1999). Cleanup requirements in these settings and throughout the United States may become more stringent in the year 2000,

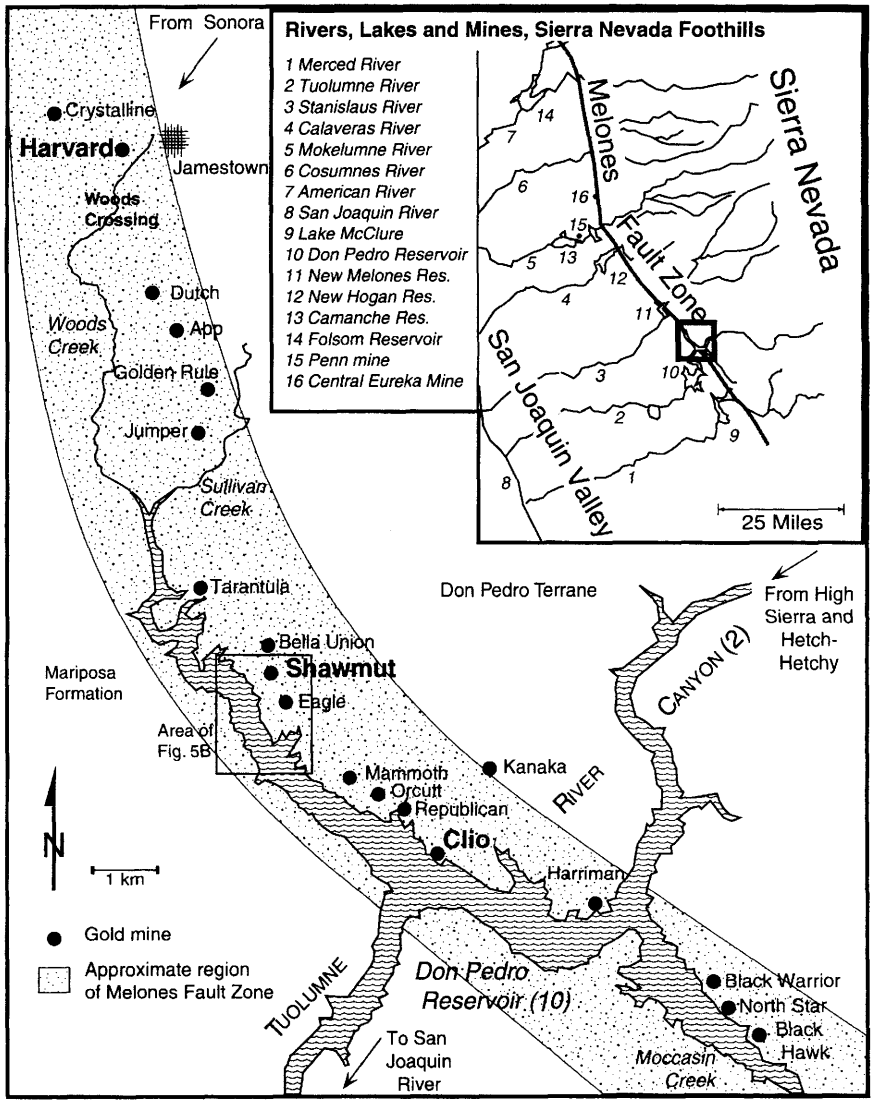

FIG. 2. Location map showing study area in relation to central and southern Mother Lode Gold District and major rivers crossing the Melones fault zone. Mine locations from Parsons (1920) and Knopf (1929). Arrows represent direction of water flow.

when the U.S. Environmental Protection Agency most likely will reduce the maximum contaminant level from its current value of 50 μg/L to a value between 2 and 20 μg/L (Pontius, 1995). It is important to ascertain sources, transport mechanisms, and sinks of arsenic in the different environments present in the Mother Lode District, both to predict the conditions under which remediation may be required, and to plan appropriate development and use of former mining lands.

This communication focuses on three distinct hydrogeologic settings within the southern Mother Lode Mining District in Tuolumne County, California (Fig. 1 inset; Fig. 2): (1) mineralized outcrops and mine waste rock (overburden), represented by pit walls of the Harvard open pit mine (Jamestown mine), outcrops near the Harriman mine, and waste rock of the Clio mine; (2) submerged mill tailings of the Eagle-Shawmut mine in Don Pedro Reservoir; and (3) lake waters in the Harvard open-pit mine

and in Don Pedro Reservoir. These environments are characterized by distinct modes of rock-water interaction that influence the local transport and fate of arsenic.

Mineralized outcrops and waste-rock piles are most influenced by seasonal extremes in the local weather. Oxidizing conditions occur during dry summers with high evaporation rates, promoting weathering of sulfide minerals. During and after winter storms, the resultant oxide and sulfate weathering products are exposed to runoff and local vadose-zone flow through joints and soil pores.

Mill tailings of the Shawmut mine are submerged beneath monomictic Don Pedro Reservoir. Sediments and porewaters near the top of the tailings piles react with lake waters, which experience seasonal changes in water chemistry. Deeper in the tailings piles, sediments and porewaters are fairly isolated from reservoir waters under typical climate conditions, but may become important sources of environmentally relevant trace metals during drought-flood cycles (El Niño, La Niña) that occur on the time scale of decades.

Lake waters in Don Pedro Reservoir and in the Harvard mine pit differ in water fluxes and in ionic strength, but both are monomictic lakes in very similar lithologic settings. The major source of water to Don Pedro Reservoir is the Tuolumne River and its watershed in the Sierra Nevada Mountains; by contrast, waters in the open-pit mine lake are evolving as the local groundwater table recovers to pre-mining conditions. Additional geochemical variations in the pit lake are imposed by seasonal rain runoff, which has interacted with the mine pit walls, and by input of waters produced by dewatering mill tailings elsewhere on the site. We examine how rock-water interactions influence the mobility of arsenic in these settings, and discuss the effects of seasonal and longer-period fluctuations in weather and climate on arsenic concentration and speciation.

Geologic Background

Regional geology

The Mother Lode Gold District of California extends for 225 km along the western Sierra Nevada foothills (Fig. 1). Most of the ore deposits formed within a folded and faulted metamorphic belt of lower greenschist- to amphibolite-facies sedimentary and igneous rocks. In the southern Mother Lode (Fig. 2), many lode gold ores are associated with the Melones fault zone, which separates a Jurassic oceanic crust complex to the west from Paleozoic metavolcanic and metasedimentary rocks to the east. The Don Pedro terrane, located between the Melones fault zone (Fig. 2) and the Sonora fault to the east (not shown), is composed of folded metasedimentary and metavolcanic rocks with mélange blocks of marble, chert, sandstone, gabbro, and serpentinite (Schweickert et al., 1988, 1999). The Jurassic Mariposa Formation is primarily slate with large lenses and blocks of serpentinized ultramafic rocks that have been further altered to talc-tremolite and chlorite-actinolite assemblages.

Ores in the southern Mother Lode formed approximately 120 Ma (Kistler et al., 1983; Bohlke and Kistler, 1986), and are classified into three belts—the Mother Lode belt, the East belt, and the West belt. They are characterized by quartz veins and carbonate rocks formed by metasomatic reaction of mineralizing fluids with greenschist-facies rocks at temperatures between 250 and 325°C (Weir and Kerrick, 1987). The ore-forming fluids introduced large quantities of CO_2, S, SiO_2, and K_2O. Tertiary uplift exposed and eroded the gold-bearing veins, forming placer deposits that were blanketed by Eocene lavas (Knopf, 1929). Continued uplift and erosion exposed the Tertiary placers and the underlying mineralized bedrock, forming modern placers whose discovery led to the California Gold Rush that began in 1848–1849.

Arsenic concentrations in gold ore of the Mother Lode are typically above 10 ppm, significantly higher than the average crustal composition of ~1 ppm (Taylor and McLennan, 1985). Figure 3A shows the relationships between bulk-rock arsenic and gold concentrations in gold ore (>1 ppm gold) in five Sierra Nevada districts (see Fig. 1). In the northern districts, where arsenopyrite is the major arsenic host mineral (Lindgren, 1896; Ferguson, 1914), arsenic concentrations are significantly higher than in the southern districts, where arsenopyrite is less common (e.g., Hodson district; see Kuhl and Lechner, 1990; Chaffee and Sutley, 1994). Mines in this study are located in the southern districts, where arsenic concentrations in ore are typically tens to several hundred parts per million (Fig. 3A) and arsenic is typically hosted in arsenian pyrite (Savage et al., 2000). Arsenic values in pyrite decrease with distance away from the Melones fault zone, from a maximum of 2.1 wt% arsenic in ore samples of the Shawmut mine to values less than 0.5

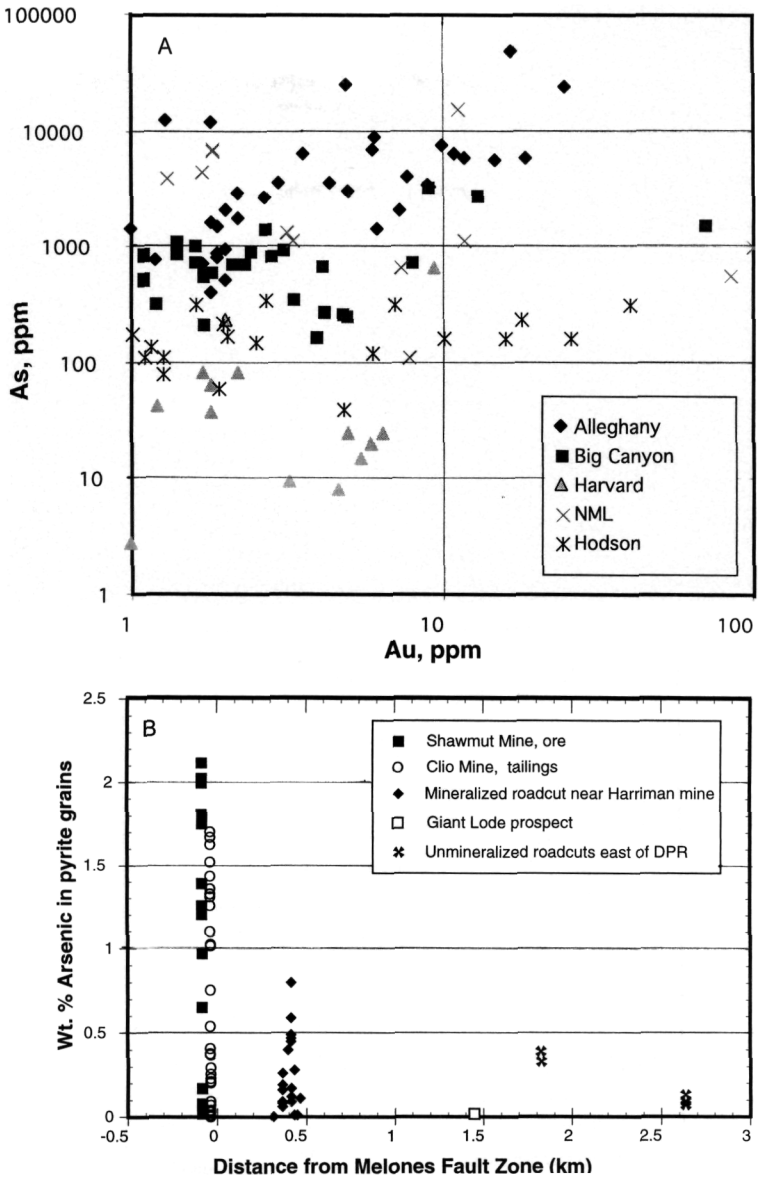

FIG. 3. A. Arsenic concentration in gold ore (>1 ppm gold) as a function of gold concentration in Mother Lode districts (see Fig. 1 for locations). B. Weight percentage of arsenic in pyrite as a function of distance from the Melones fault zone. Zero on the horizontal axis marks the approximate center of the Melones fault zone where samples from the Clio and Shawmut mines are plotted. The distance +0.5 km denotes the eastern edge of the fault zone; the samples here are from a mineralized outcrop near the Harriman mine (see Fig. 2). Each data point represents the average of 3 to 9 electron microprobe analyses of a single pyrite grain. Abbreviations: NML = mines of the northern Mother Lode including Sutter Creek, Nashville, Georgetown, Spanish Flat, Kelsey, and Nevada City districts; DPR = Don Pedro Reservoir.

wt% arsenic in samples collected one to three kilometers away, as illustrated in Figure 3B (Savage et al., 2000).

Mine site history and geology

The Harvard lode (Fig. 1 inset; Fig. 2), part of the Jamestown mine, was discovered in 1850 and

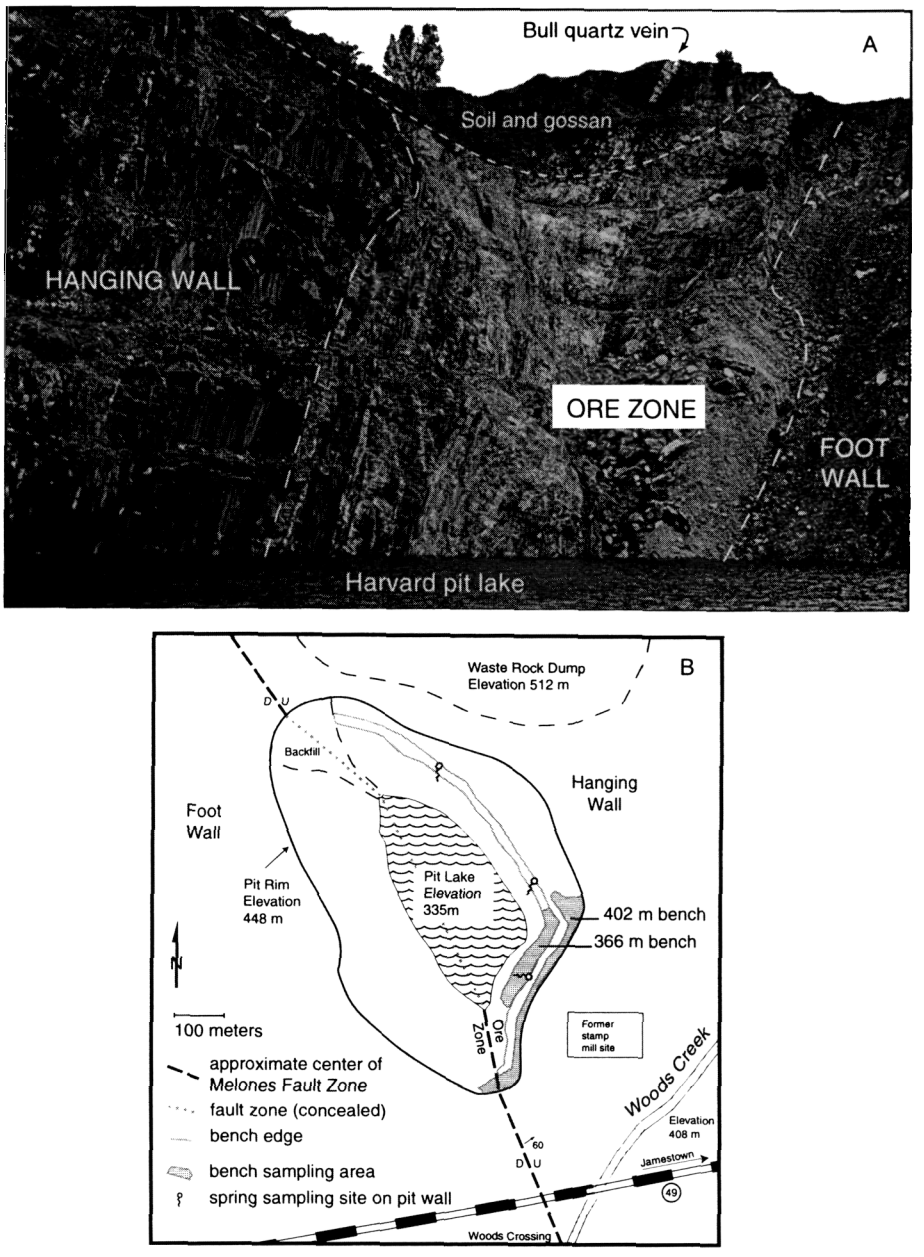

FIG. 4. A. View to southeast in the Harvard open-pit mine including lake and pit walls. Hanging wall is composed primarily of slates; footwall is "serpentinites" altered to talc-tremolite and chlorite-actinolite schists, and the ore zone is sheared slices of hanging-wall and footwall rocks and altered dikes. B. Map of the Harvard open pit mine in relation to the Melones fault zone, Woods Creek, and Highway 49, showing locations of springs, sampled benches, and the pit lake.

worked continuously from 1899 to 1916, supporting a 60-stamp mill; it was reopened briefly from 1938 to 1942 (Allgood, 1990). Between 1987 and July 1994, the Sonora Mining Company developed open-pit excavations at the Harvard (Fig. 4) and nearby Crystalline deposits, producing more than 600,000 troy ounces of gold and excavating the 25.8 kg "Christmas nugget" in 1992 (Nelson and Leicht,

1994). Mineralization at the Harvard is concentrated along the Melones fault zone (Fig. 4; Landefeld and Snow, 1990). The southwest portion of the pit (footwall; Fig. 4) is composed of greenschist-facies mafic and ultramafic igneous rocks altered to chlorite-actinolite and talc-tremolite schists. The northeast area of the pit (hanging wall) is composed of interlayered graphitic slate, metavolcanic and metavolcaniclastic rocks, and schists. Gold ore consists of an extensively sheared and altered mélange of hanging- and footwall rocks that include ankerite schist, ankeritic banded slate, metavolcanic greenstone, chlorite schist, talc schist, quartz-ankerite-mariposite rock, sericite schist, and altered dikes (Dohms et al., 1985; Allgood et al., 1987; Landefeld and Snow, 1990). Alteration mineralogy and parageneses are characterized by intense CO_2 metasomatism and varying degrees of albitization, sericitization, and silicification associated with numerous vein sets.

The Eagle-Shawmut mine (Jacksonville District of Figure 1; Figs. 2, 5) was the largest in Tuolumne County (Clark, 1970; Wagner, 1970), operating intermittently until 1947. It produced 2.8 million tons of ore and $7.4 million worth of gold, and supported a 100-stamp mill. The predominantly sulfide-rich ore included up to 15% pyrite and arsenopyrite, unusual among Mother Lode deposits that typically contained only a few percent sulfide (Knopf, 1929). The mine workings extended to 4500 feet and sulfide-rich ore continued to depth. From 1942 to 1947, copper ore from the Pen mine, a massive-sulfide deposit in Calaveras County (Fig. 2, inset point 15), was processed at the Eagle-Shawmut mill (the Penn mine recently has been the site of extensive efforts to remediate leakage of acid mine waters into Camanche Reservoir; Hunerlach and Alpers, 1994). The Clio mine (Fig. 2) was considerably smaller than the Eagle-Shawmut, with only a 10-stamp mill, but host-rock lithologies and structural relations are similar (Knopf, 1929). Gold is mostly disseminated in pyrite but free specimen gold also was found; there is no mention of arsenopyrite in the mine description (Knopf, 1929). In 1970, the processing facilities and tailings of the Eagle-Shawmut mine and the tailings of the Clio mine were submerged by the newly expanded Don Pedro Reservoir. Figure 5 indicates the present high-water shoreline (white line) on a 1914 photograph of the Shawmut mill and tailings piles.

Methods

Outcrops

Rock samples were collected from outcrops and analyzed by X-ray diffraction (CuKα radiation, Stanford University), electron probe microanalysis (EPMA; details in Tables 1–4), X-ray fluorescence (XRF; Chemex Laboratories, Sparks, NV), and inductively coupled plasma–atomic emission spectrometry (ICP-AES; Chemex Laboratories). Analyses presented in Figure 3 were performed by fire assay–atomic absorption (FA-AA) for Au, and by atomic absorption spectroscopy (AAS) for As at Chemex Laboratories.

Submerged tailings

Gravity cores of submerged tailings were collected during October 1997 and June 1998 from a sled boat with motorized winch, employing 10 cm x 1 m polycarbonate core tubes. Cores were capped at both ends, placed upright into an ice container, and transported to the U.S. Geological Survey in Sacramento. Cores were photographed, demarcated into layers based on sediment color and texture, and extruded under a nitrogen or argon gas atmosphere. The extruder pushes the core up into a glove bag by means of an inert-gas "hydraulic" device, with rate of extrusion controlled by the gas flow beneath a plug at the core's base. Minor disturbance to the cores typically resulted from inert gas bubbles entering the core from beneath the plug. In the inert atmosphere, discrete layers of sediment were scraped or spooned into 250 mL polycarbonate centrifuge tubes. Samples were centrifuged (20 to 30 minutes, angular velocity 17,000 RPM) and transferred into a nitrogen or argon atmosphere for porewater extraction. Solids were analyzed as described above for rock samples.

Porewaters were drawn by syringe from the centrifuge tubes and filtered to 0.45 μm. Subsamples for metal concentrations by ICP-MS (Chemex Laboratories, Sparks NV or Actlabs Inc., Wheat Ridge, CO) were acidified with Ultrex HNO_3; subsamples for arsenic and iron speciation (Frontier Geosciences, Seattle, WA) were acidified to pH < 2 with Ultrex HCl and kept at 4°C until analysis. Subsamples for alkalinity determination (by Gran multipoint method) were kept on ice until titrations could be performed (typically within 8 to 24 hours of sample collection). Major anion analysis was performed at the Division National Water Quality Laboratory Unit (Ocala, FL).

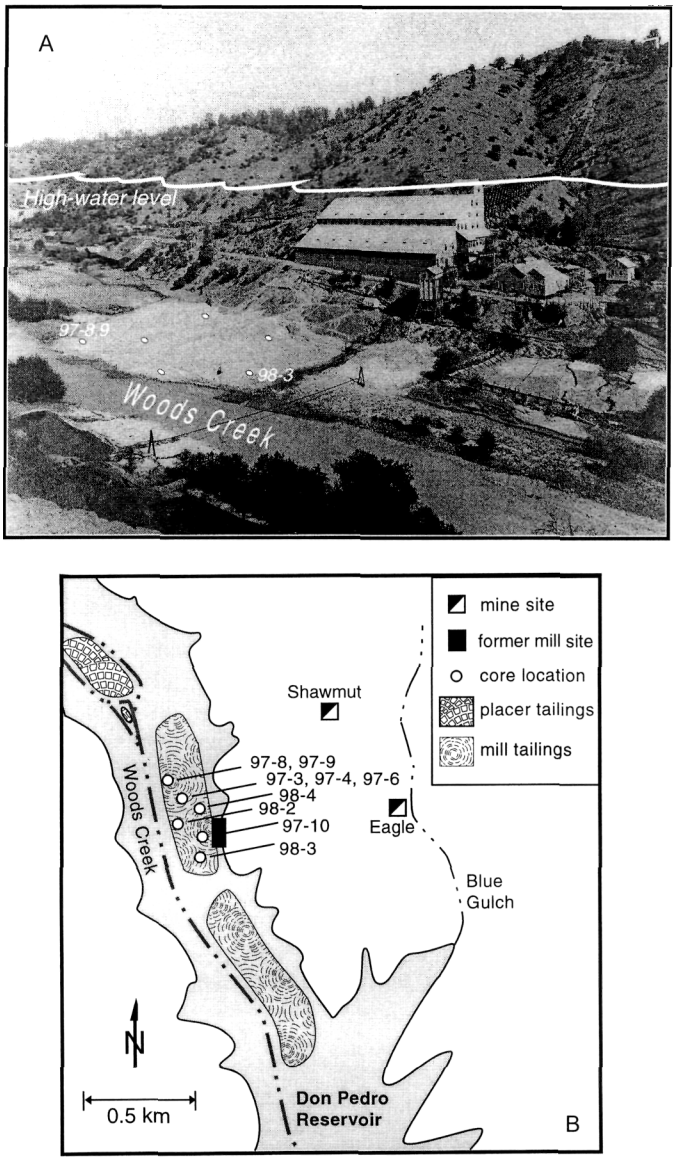

FIG. 5. A. View to NNE of the Shawmut mill in 1914 (see Fig. 2; photo courtesy of Tuolumne County Museum) showing the present high-water level of Don Pedro Reservoir and approximate locations of sediment cores in mill tailings. B. Map of the Eagle-Shawmut study area, showing approximate locations of tailings piles (interpreted from 1945 aerial photographs) and sediment cores relative to the present high-water level of Don Pedro Reservoir.

Lake waters

Water samples were collected from various lake depths in a vertical Kemmerer-style sampler. Subsamples were processed immediately by filtration (0.45 pm) and/or acidification, and analyzed as described above for tailings porewaters. Temperature, pH, and dissolved oxygen measurements for vertical depth profiles were collected using a HydrolabTM Minisonde Multiprobe calibrated with pH 4 and 7 buffer solutions. Dissolved oxygen was calibrated assuming 100% saturation in lake surface water (0.1 m depth) at the measured barometric pressure.

TABLE 1. Results of Electron-Probe Microanalysis, Margins of the Melones Fault Zone Mélange

Sample:	DP-007		DP- 027		DP-032		DP-033		DP- 035		DP-077		DP-078		DP-083	
No. analyses:	5	*SD*	5	*SD*	3	*SD*	5	*SD*	5	*SD*	5	*SD*	4	*SD*	5	*SD*
Fe	47.12	0.15	46.96	0.23	46.95	0.15	46.89	0.24	47.11	0.23	47.08	0.24	47.03	0.14	46.89	0.11
S	52.91	0.55	52.46	0.39	52.29	0.54	52.90	0.77	52.99	0.30	52.46	0.45	52.39	0.25	53.03	0.65
As	0.06	0.11	0.00	0.01	0.28	0.11	0.01	0.01	0.01	0.01	0.08	0.08	0.11	0.08	0.40	0.11
Zn	0.01	0.01	0.01	0.01	0.00	0.01	0.01	0.01	0.01	0.01	0.02	0.02	0.01	0.01	0.01	0.01
Pb	0.01	0.01	0.01	0.01	0.04	0.03	0.02	0.03	0.01	0.01	0.01	0.01	0.03	0.03	0.05	0.04
Mn	0.01	0.01	0.01	0.01	0.01	0.01	0.01	0.01	0.01	0.01	0.01	0.01	0.01	0.01	0.02	0.01
Sb	0.01	0.00	0.01	0.01	0.01	0.01	0.01	0.00	0.01	0.00	0.01	0.00	0.01	0.01	0.01	0.01
Cu	0.04	0.02	0.01	0.00	0.01	0.01	0.01	0.00	0.01	0.01	0.01	0.00	0.01	0.01	0.01	0.01
Bi	0.01	0.01	0.00	0.01	0.01	0.01	0.00	0.01	0.00	0.00	0.01	0.01	0.01	0.01	0.02	0.03
Co	0.09	0.00	0.10	0.01	0.10	0.02	0.09	0.02	0.10	0.01	0.09	0.03	0.09	0.01	0.11	0.00
Ni	0.12	0.06	0.04	0.02	0.05	0.04	0.03	0.02	0.02	0.01	0.04	0.01	0.04	0.02	0.03	0.01
Se	0.00	0.01	0.00	0.00	0.01	0.01	0.00	0.00	0.00	0.01	0.00	0.00	0.00	0.01	0.00	0.01
Totals	100.38		99.63		99.74		99.98		100.28		99.81		99.73		100.58	

[1]Analyses conducted on a JEOL 733 fully automated Superprobe with five wavelength-dispersive spectrometers. Operating conditions were 15 keV acceleration potential and 50 nA beam current, with a spot size of 1 μm. Count times were 1 second. Data acquisition utilized the MAN background correction procedure of Donovan and Tingle (1996). Background-corrected X-ray intensity measurements were analyzed using a ZAF/phi-rho-Z matrix correction procedure (Pouchou and Pichoir, 1985). Analyses are given in weight percent. Number of analyses contributing to each average is given below the sample name. Detection limits for iron, sulfur, and arsenic were approximately 0.1 wt%. Synthetic sulfide standards were from the Czamanske collection (U.S. Geological Survey).

TABLE 2. Results of Electron-Probe Microanalysis, Mineralized Calaveras Formation[1]

Sample:	DP-038 Fe-Ox		DP-038 py inclusions	
No. analyses:	5	*SD*	2	*SD*
Fe	88.13	1.63	47.60	0.95
S	0.03	0.02	52.90	0.25
As	0.20	0.05	0.02	0.02
Zn	0.01	0.00	0.02	0.01
Pb	0.00	0.00	0.01	0.01
Mn	0.03	0.01	0.01	0.01
Sb	0.01	0.01	0.01	0.01
Cu	0.13	0.05	0.01	0.01
Bi	0.01	0.01	0.00	0.00
Co	0.22	0.02	0.26	0.25
Ni	0.05	0.03	0.03	0.01
Se	0.01	0.01	0.00	0.00
Totals	98.96		100.87	

[1]For procedure, see Note 1, Table 1.

Results

Outcrop sources of arsenic

Arsenic is concentrated in mineralized rocks of the Melones fault zone relative to rocks outside the fault zone, which have been metamorphosed but have not experienced significant interaction with mineralizing fluids (see Fig. 3B; Savage et al., 2000). Of the rock types present in the field study area (Fig. 2), the highest arsenic concentrations are present in albite-chlorite schists of the Clio mine and nearby outcrops, and in footwall rocks of the Harvard mine, which are composed of talc-tremolite and chlorite-actinolite assemblages (after serpentine). There is a moderate positive correlation between arsenic and iron in the Melones fault zone rocks and their weathering products (Fig. 6). The highest arsenic concentrations are in pyrite-bearing rocks and in weathering products commonly associated with pyrite. Microprobe analyses confirm the presence of arsenic in pyrite (Tables 1–4), and also demonstrate that there are no other modally abundant minerals containing arsenic in the study area. However, there are trace quantities of the arsenic minerals niccolite (NiAs), cobaltite (COASS), and gersdorffite (NiAsS) in some rocks of ultramafic derivation. Cobaltite also is present as inclusions within pyrite in albite-chlorite schists of the Clio mine.

Individual pyrite grains contain up to ~4 wt% arsenic (averages typically <2 wt%). Figures 7A and 7B show arsenic-concentration contour maps of two pyrite grains from albite-chlorite schist of the Clio mine waste-rock pile. Each map is generated from approximately 8000 finely spaced (10 to 20 μm) electron microprobe analyses. Arsenic concentrations are represented on the histograms in Figures 7C and 7D. Less than 0.05% of the analyses are arsenopyrite inclusions (not shown in the range of the histograms). The microprobe data, together with high-resolution transmission electron microscopy and arsenic K-edge extended X-ray absorption fine structure spectroscopy (EXAFS), indicate that arsenic in pyrite occurs in solid solution replacing sulfur, not as inclusions or layers of other arsenic phases (Savage et al., 2000). Arsenic in pyrite from the Harvard mine (Figs. 7E and 7F) shows a somewhat different distribution than in pyrite from the Clio mine; here arsenic is concentrated in thin, undulating zones that also are rich in nickel. Figures 7D and 7F are backscattered electron microprobe images of a pyrite grain from coarse granular albite-ankerite schist of the Harvard mine hanging-wall ore zone, in which the arsenic-rich regions

TABLE 3. Results of Electron-Probe Microanalysis, Shawmut Mine[1]

Location:	8215.2		8215.3		8215.4		8215.5		8215.6		8215.7		8215.8		8215.9		8215.10		8215.12	
No. analyses:	7	*SD*	7	*SD*	9	*SD*	3	*SD*	6	*SD*	4	*SD*	5	*SD*	4	*SD*	4	*SD*	4	*SD*
Fe	45.96	0.33	46.39	0.31	46.22	0.46	46.21	0.07	46.94	0.18	46.40	0.30	46.65	0.10	45.81	0.57	46.04	0.27	46.19	0.70
S	50.69	1.39	52.15	0.94	51.83	0.94	52.67	0.95	53.05	0.48	52.47	0.43	52.73	0.39	52.58	0.41	51.68	1.18	53.37	0.92
As	2.12	0.53	1.75	0.54	2.00	0.34	1.39	0.22	0.17	0.40	0.97	0.67	1.21	0.37	0.65	0.98	1.81	0.46	0.02	0.01
Zn	0.00	0.01	0.01	0.02	0.01	0.01	0.00	0.01	0.02	0.02	0.00	0.00	0.01	0.02	0.00	0.00	0.02	0.02	0.01	0.02
Pb	0.09	0.15	0.16	0.11	0.05	0.09	0.19	0.33	0.00	0.01	0.06	0.07	0.05	0.07	0.02	0.03	0.24	0.19	0.01	0.02
Mn	0.00	0.00	0.01	0.01	0.00	0.01	0.02	0.02	0.00	0.00	0.00	0.00	0.00	0.00	0.00	0.00	0.01	0.01	0.01	0.01
Sb	0.01	0.01	0.00	0.01	0.01	0.01	0.02	0.02	0.02	0.02	0.00	0.00	0.00	0.01	0.00	0.00	0.00	0.00	0.00	0.00
Cu	0.00	0.01	0.00	0.01	0.01	0.02	0.00	0.00	0.01	0.02	0.00	0.00	0.00	0.00	0.01	0.01	0.00	0.00	0.00	0.00
Bi	0.00	0.00	0.00	0.00	0.00	0.00	0.00	0.00	0.00	0.00	0.04	0.05	0.02	0.03	0.00	0.00	0.00	0.00	0.00	0.00
Co	0.09	0.06	0.07	0.04	0.05	0.02	0.06	0.04	0.04	0.01	0.04	0.02	0.05	0.01	0.05	0.01	0.05	0.03	0.05	0.01
Ag	0.02	0.02	0.01	0.01	0.02	0.03	0.01	0.01	0.01	0.02	0.02	0.02	0.01	0.02	0.00	0.00	0.02	0.02	0.00	0.00
Ni	0.00	0.01	0.01	0.01	0.02	0.02	0.01	0.01	0.00	0.00	0.00	0.00	0.01	0.02	0.01	0.01	0.01	0.01	0.00	0.00
Au	0.02	0.03	0.01	0.01	0.01	0.02	0.00	0.00	0.01	0.02	0.00	0.00	0.03	0.06	0.01	0.01	0.01	0.02	0.00	0.01
Totals	99.02		100.57		100.22		100.57		100.27		100.01		100.77		99.13		99.88		99.66	

(*continued*)

TABLE 3. (continued)

Location:	8215.14		8215.17		8215.19		8215.21	
No. analyses:	2	*SD*	1	*SD*	3	*SD*	5	*SD*
Fe	46.75	0.15	46.33	n.a.	46.44	0.22	46.45	0.27
S	52.26	1.11	52.22	n.a.	53.46	0.70	52.39	0.49
As	1.20	1.70	2.02	n.a.	0.08	0.13	1.39	0.70
Zn	0.02	0.02	0.00	n.a.	0.02	0.04	0.03	0.03
Pb	0.07	0.10	1.78	n.a.	0.29	0.26	0.17	0.15
Mn	0.01	0.01	0.00	n.a	0.00	0.00	0.00	0.00
Sb	0.00	0.00	0.00	n.a.	0.01	0.01	0.00	0.01
Cu	0.03	0.04	0.00	n.a.	0.07	0.09	0.00	0.00
Bi	0.00	0.00	0.00	n.a.	0.00	0.00	0.00	0.00
Co	0.06	0.02	0.05	n.a.	0.07	0.01	0.06	0.02
Ag	0.03	0.01	0.04	n.a.	0.02	0.03	0.04	0.03
Ni	0.00	0.00	0.00	n.a.	0.01	0.02	0.01	0.02
Au	0.04	0.05	0.00	n.a.	0.03	0.05	0.00	0.00
Totals	101.06		102.43		100.51		101.03	

[1]For procedure, see note 1, Table 1.

appear as bright lines (indicated by white arrows in Fig. 7F).

Secondary mineral sinks for arsenic

Arsenic is concentrated in fine-grained, friable, iron-rich weathering products of arsenian pyrite (Fig. 6), which develop as efflorescences and crusts on weathering outcrops. Arsenic is primarily associated with goethite (α-Fe00H), jarosite ($KFe_3(SO_4)_2(OH)_6$), and copiapite ($Fe(II)Fe(III)_4(SO_4)_6(OH)_2 \cdot 20(H_2O)$). Up to ~1300 ppm arsenic is found in goethite-rich weathering crusts on the Clio mine tailings (samples DP-001, DP-011, DP-112) and in jarosite-rich weathering crusts on mineralized outcrops (samples DP-045, DP-047). Two samples of copiapite efflorescences from the Harvard mine (south end of pit, 402 m bench, see Fig. 4) contain approximately 300 ppm arsenic (samples HP-019, HP-045). Jarosite at the Harvard mine develops primarily on joint surfaces of graphite-rich (>1%) black slates. Three samples of slate with jarosite contain 70 to 150 ppm arsenic, while a goethite-rich sample (HP-023) contains 722 ppm arsenic. The highest arsenic contents of the Harvard mine weathering products, 800 to 1260 ppm, were found in pyritic quartz-magnesite-mariposite rocks with efflorescences of gypsum ($CaSO_4 \cdot 2H_2O$) and hexahydrite ($MgSO_4 \cdot 6H_2O$) within the ore zone (HP-014, HP-015).

The bonding environment of arsenic in selected natural samples from the Clio mine and an outcrop near the Harriman mine was evaluated by arsenic K-edge EXAFS (Savage et al., 2000). In goethite-rich samples, arsenic is present as the As(V) oxyanion (arsenate) adsorbed to goethite in a bidentate mode, consistent with laboratory studies by Waychunas et al. (1993, 1995). For jarosite-rich samples, EXAFS spectra were consistent with arsenate substitution for sulfate in the jarosite structure. Such a substitution has been proposed in other natural samples (Foster et al., 1998; Huggins et al., 1997) and synthetic jarosites (Dutrizac and Jambor, 1987; Dutrizac et al., 1987).

Submerged mill tailings and porewaters

Figure 5A shows the Eagle-Shawmut mine and its 100-stamp mill in 1914. The light-colored tailings pile in the left foreground as well as the tailings pond in the lower right are both clearly larger on 1945 aerial photographs. The present high-water level (253 m elevation) of Don Pedro Reservoir is indicated on the photograph by a white line. The locations of the tailings piles beneath the present water surface were ascertained by acoustic depth

TABLE 4. Results of Electron-Probe Microanalysis, Clio Mine Tailings Pile[1]

Location:	Clio-1.1		Clio-1.2		Clio-1.3		Clio-1.4		Clio-2.1	
No. analyses:	5	*SD*	3	*SD*	3	*SD*	3	*SD*	4	*SD*
Fe	47.56	0.47	47.58	0.45	46.63	0.41	47.62	0.34	45.90	0.44
S	53.01	0.96	53.60	0.50	53.21	0.10	53.34	0.62	52.41	0.49
As	0.09	0.12	0.00	0.00	0.03	0.05	0.07	0.12	0.75	0.41
Zn	0.00	0.00	0.01	0.02	0.00	0.00	0.00	0.00	0.01	0.01
Pb	0.00	0.00	0.03	0.06	0.00	0.00	0.01	0.02	0.18	0.27
Mn	0.00	0.00	0.01	0.01	0.00	0.00	0.00	0.00	0.01	0.01
Sb	0.00	0.00	0.01	0.01	0.00	0.00	0.00	0.00	0.01	0.02
Cu	0.00	0.00	0.00	0.00	0.01	0.01	0.01	0.01	0.01	0.02
Bi	0.00	0.00	0.03	0.05	0.00	0.00	0.00	0.00	0.00	0.00
Co	0.10	0.05	0.10	0.02	0.21	0.17	0.08	0.06	0.06	0.03
Ag	0.01	0.03	0.00	0.01	0.02	0.03	0.02	0.04	0.02	0.03
Ni	0.08	0.09	0.03	0.04	0.12	0.02	0.02	0.03	0.00	0.00
Au	0.00	0.01	0.02	0.04	0.01	0.01	0.01	0.02	0.01	0.01
Totals	100.86		101.43		100.24		101.18		99.38	

Location:	Clio-2.2		Clio-2.3		Clio-2.4		Clio-2.5		Clio-2.8	
No. analyses:	9	*SD*	5	*SD*	6	*SD*	6	*SD*	3	*SD*
Fe	45.78	0.54	45.57	0.13	45.84	0.13	45.42	0.26	46.72	0.18
S	51.91	0.44	52.60	1.16	52.71	0.43	52.58	1.57	57.55	1.47
As	1.33	0.73	1.26	0.40	1.02	0.84	1.36	0.26	0.00	0.00
Zn	0.02	0.03	0.01	0.01	0.00	0.00	0.01	0.01	0.00	0.00
Pb	0.12	0.12	0.29	0.34	0.24	0.27	0.12	0.10	0.00	0.00
Mn	0.00	0.00	0.01	0.01	0.01	0.01	0.01	0.01	0.01	0.01
Sb	0.00	0.01	0.01	0.01	0.00	0.01	0.00	0.00	0.01	0.01
Cu	0.00	0.01	0.00	0.00	0.00	0.00	0.01	0.02	0.04	0.04
Bi	0.00	0.00	0.00	0.01	0.01	0.02	0.03	0.04	0.00	0.00
Co	0.08	0.05	0.05	0.02	0.04	0.01	0.07	0.05	0.05	0.01
Ag	0.01	0.02	0.03	0.04	0.01	0.01	0.01	0.02	0.00	0.00
Ni	0.05	0.09	0.00	0.00	0.00	0.00	0.02	0.04	0.01	0.01
Au	0.01	0.03	0.01	0.01	0.00	0.00	0.00	0.00	0.02	0.03
Totals	99.31		99.84		99.88		99.64		104.40	

Location:	Clio-2.9		Clio-2.10		Clio-2.11		Clio-2.12		Clio-2.16	
No. analyses:	4	*SD*	7	*SD*	6	*SD*	5	*SD*	5	*SD*
Fe	45.95	0.09	46.62	0.32	46.27	0.30	46.44	0.27	47.03	0.31
S	57.16	2.17	59.67	1.68	56.48	1.91	57.04	1.71	52.32	0.53
As	1.63	0.44	1.03	0.75	1.44	0.29	1.52	0.75	1.33	0.41
Zn	0.02	0.02	0.00	0.01	0.01	0.01	0.00	0.00	0.00	0.00
Pb	0.25	0.18	0.27	0.21	0.18	0.21	0.33	0.24	0.29	0.25
Mn	0.00	0.01	0.01	0.01	0.01	0.01	0.01	0.01	0.01	0.01
Sb	0.00	0.01	0.00	0.01	0.01	0.01	0.02	0.03	0.01	0.01
Cu	0.00	0.00	0.09	0.17	0.00	0.01	0.01	0.02	0.01	0.01
Bi	0.01	0.01	0.00	0.00	0.00	0.01	0.00	0.00	0.00	0.00
Co	0.05	0.04	0.06	0.03	0.04	0.01	0.05	0.02	0.07	0.01
Ag	0.01	0.03	0.02	0.04	0.08	0.07	0.03	0.06	0.02	0.03
Ni	0.00	0.00	0.01	0.02	0.00	0.01	0.00	0.00	0.01	0.02
Au	0.01	0.02	0.04	0.06	0.02	0.03	0.00	0.00	0.02	0.03
Totals	105.11		107.82		104.55		105.46		101.10	

(*continued*)

TABLE 4. (*continued*)

Location:	Clio-2.18		Clio-2.19		Clio-3.1		Clio-3.2		Clio-3.3	
No. analyses:	5	*SD*	5	*SD*	6	*SD*	7	*SD*	5	*SD*
Fe	47.01	0.22	46.82	0.30	46.60	0.35	46.25	0.15	46.32	0.30
S	52.23	0.24	52.04	0.33	55.84	2.21	57.07	2.47	57.46	2.22
As	1.70	0.22	1.67	0.48	0.29	0.24	0.26	0.27	0.23	0.24
Zn	0.01	0.02	0.00	0.01	0.02	0.02	0.00	0.00	0.01	0.01
Pb	0.20	0.23	0.16	0.06	0.04	0.06	0.03	0.04	0.05	0.06
Mn	0.01	0.01	0.01	0.01	0.00	0.00	0.01	0.01	0.00	0.00
Sb	0.00	0.00	0.00	0.00	0.00	0.00	0.02	0.02	0.01	0.02
Cu	0.00	0.01	0.00	0.01	0.00	0.00	0.00	0.00	0.00	0.00
Bi	0.00	0.00	0.00	0.00	0.00	0.00	0.01	0.02	0.00	0.00
Co	0.08	0.03	0.07	0.02	0.04	0.02	0.05	0.02	0.04	0.01
Ag	0.02	0.02	0.02	0.02	0.03	0.03	0.03	0.03	0.01	0.01
Ni	0.02	0.02	0.02	0.01	0.00	0.00	0.00	0.00	0.00	0.01
Au	0.02	0.03	0.01	0.01	0.02	0.05	0.01	0.02	0.00	0.00
Totals	101.30		100.82		102.90		103.73		104.13	

Location:	Clio-3.4		Clio-3.5		Clio-3.6		Clio-3.7		Clio-3.8	
No. analyses:	7	*SD*	5	*SD*	6	*SD*	6	*SD*	6	*SD*
Fe	45.86	0.27	46.17	0.33	46.33	0.22	46.09	0.21	45.89	0.57
S	55.12	2.07	53.62	0.74	54.32	1.39	53.86	1.05	53.44	1.89
As	0.03	0.06	0.37	0.58	1.10	0.31	0.20	0.34	0.54	0.97
Zn	0.01	0.02	0.00	0.01	0.01	0.02	0.00	0.01	0.02	0.04
Pb	0.06	0.06	0.02	0.05	0.07	0.08	0.03	0.05	0.01	0.02
Mn	0.01	0.01	0.01	0.01	0.00	0.00	0.00	0.00	0.01	0.01
Sb	0.01	0.03	0.02	0.04	0.00	0.00	0.02	0.03	0.00	0.00
Cu	0.00	0.00	0.01	0.02	0.00	0.00	0.01	0.01	0.03	0.04
Bi	0.00	0.00	0.00	0.00	0.00	0.01	0.03	0.05	0.00	0.00
Co	0.05	0.02	0.06	0.02	0.05	0.01	0.04	0.02	0.04	0.02
Ag	0.02	0.02	0.00	0.01	0.01	0.03	0.02	0.03	0.01	0.02
Ni	0.01	0.02	0.00	0.00	0.00	0.00	0.01	0.01	0.01	0.01
Au	0.00	0.01	0.01	0.01	0.01	0.02	0.01	0.02	0.01	0.02
Totals	101.19		100.29		101.91		100.32		100.00	

Location:	Clio-3.9		Clio-3.10		Clio-3.11		Clio-3.14	
No. analyses:	5	*SD*	1	*SD*	3	*SD*	2	*SD*
Fe	45.87	0.37	47.09	n.a.	46.59	0.29	47.48	0.17
S	53.11	2.07	53.03	n.a.	53.14	0.64	52.77	0.28
As	0.03	0.04	0.03	n.a.	0.41	0.31	0.01	0.01
Zn	0.01	0.02	0.00	n.a.	0.05	0.04	0.00	0.00
Pb	0.01	0.02	0.09	n.a.	0.05	0.09	0.08	0.10
Mn	0.02	0.02	0.00	n.a.	0.00	0.00	0.00	0.00
Sb	0.01	0.03	0.00	n.a.	0.00	0.01	0.01	0.02
Cu	0.04	0.06	0.00	n.a.	0.02	0.03	0.00	0.00
Bi	0.00	0.00	0.00	n.a.	0.00	0.00	0.00	0.00
Co	0.06	0.03	0.04	n.a.	0.06	0.00	0.04	0.01
Ag	0.06	0.06	0.01	n.a.	0.02	0.02	0.08	0.00
Ni	0.00	0.01	0.01	n.a.	0.02	0.02	0.03	0.00
Au	0.00	0.00	0.08	n.a.	0.02	0.03	0.00	0.00
Totals	99.22		100.38	n.a.	100.38		100.50	

[1]For procedure, see Note 1, Table 1.

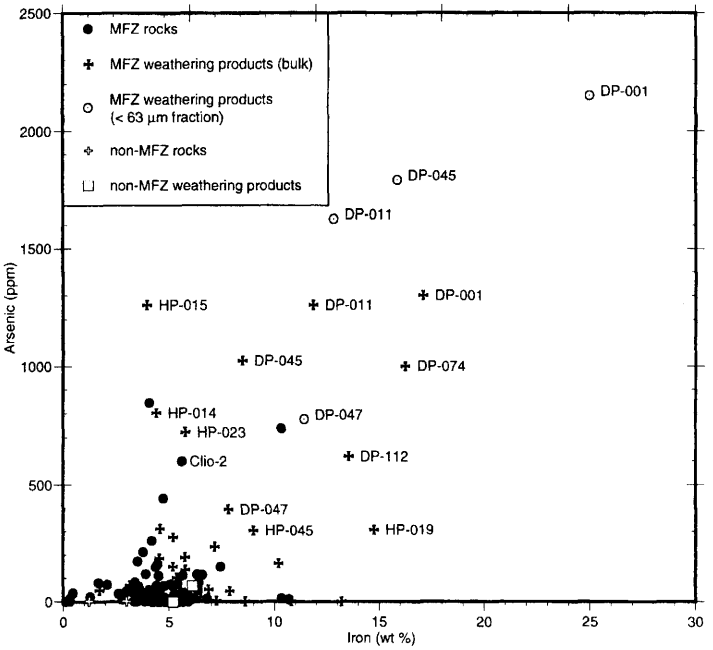

FIG. 6. Arsenic concentration in rocks, outcrops, and mine tailings as a function of weight percentage iron. Most Melones fault zone (MFZ) samples are from the Harvard and Clio mines. Analyses of Shawmut mill tailings and overlying lake sediments are shown in Figue 8.

finder and visual comparisons with the historic and aerial photographs. Cores were collected only from the upstream pile (Fig. 5B), because a hardpan layer prohibited penetration of the gravity-coring device in the downstream pile. Core recovery typically included 15 to 45 cm of sediment and 20 to 40 cm of lake water. In all cores except 98-4 the uppermost sediment layer was a dark brown organic-rich mud. Core 98-3 included only a mud layer, while core 98-4 was primarily sand. In cores 97-3, 97-4, 97-6, 97-10, and 98-2, the layer beneath the mud consisted of fine-grained sand or silt identified as mill tailings. In some of these cores, this layer was finely laminated, with ~1 mm thick bands of grey alternating with yellow, or yellow alternating with orange tailings. In cores 97-8 and 97-9, the surface mud was underlain by coarser, yellow-brown sand. X-ray diffraction and scanning electron microscopy with energy-dispersive X-ray analysis of core subsamples indicates that the major minerals in the upper lake muds are quartz, orthoclase, and chlorite. The coarse sands are composed primarily of quartz and gypsum and the fine tailings contain mostly quartz with minor gypsum, plus chlorite in the grey samples. Grains in the three samples examined by SEM (mud and coarse sand of core 97-9, and fine yellow tailings of core 97-3) have patchy aggregates of fine iron oxides or hydroxides on their surfaces, along with much finer (<10 gm) quartz and feldspar grains.

Table 5 presents bulk chemical analyses of the core samples. Distinct chemical signatures with regard to arsenic and mercury are evident among the different sediment types within the cores (Fig. 8A). Both arsenic and mercury concentrations in the upper mud layers of the cores are low relative to deeper layers, with arsenic values of 50 to 70 ppm and mercury values of 0.5 to 1.1 ppm. Arsenic concentrations in the coarse sand layers are highest but also cover the broadest range, from 115 to 300 ppm. The fine yellow to orange tailings are intermediate in arsenic concentrations (80 to 170 ppm), but have the highest mercury values, between 2 and 3.5 ppm (Fig. 8A). There is not a distinct base-metal signature among the different sediment groups; the sum of lead, zinc, copper, cadmium, cobalt, and nickel is typically in the 1000 to 2000 ppm range (Fig. 8B). In most samples zinc is the predominant base metal. Lead dominates in samples of core 97-10, and copper dominates in only one sample (the base of core

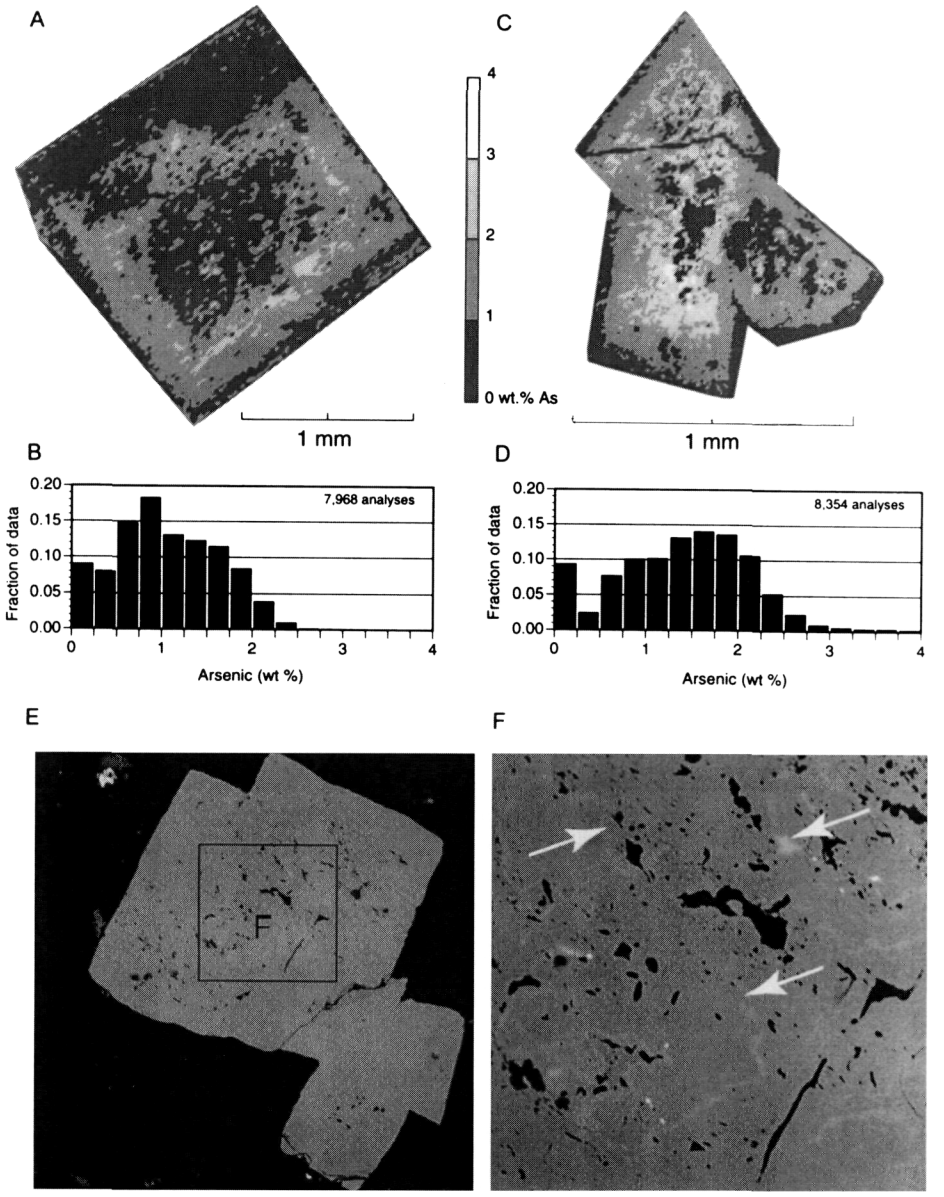

FIG. 7. A-D. Concentration maps and histograms of arsenic concentration in two pyrite grains (A, B, 7968 analyses of Crystal l; C, D, 8354 analyses of Crystal 2), from albite-chlorite schist of the Clio mine (sample Clio-2). Analyses by electron microprobe on 10 to 20 μm rectangular grid. E-F. Backscattered electron images of pyrite from coarse granular albite-ankerite schist of the Harvard mine hanging-wall ore zone. Thin undulating arsenic-rich regions appear as bright lines (arrows in F).

97-6). A few individual samples of coarse sand and fine tailings have much higher base-metal concentrations, up to 7000 ppm. Sediments collected from atop base-metal slag piles at the Penn mine (Fig. 2, inset) have similar base-metal concentrations, from 650 to 1730 ppm in silty sands and 6300 pm in mud (Parsons et al., 2000), whereas sediments downstream from the Penn mine in Camanche Reservoir have lower concentrations (less than 400 ppm; Slotton and Reuter, 1995). The high concentrations of

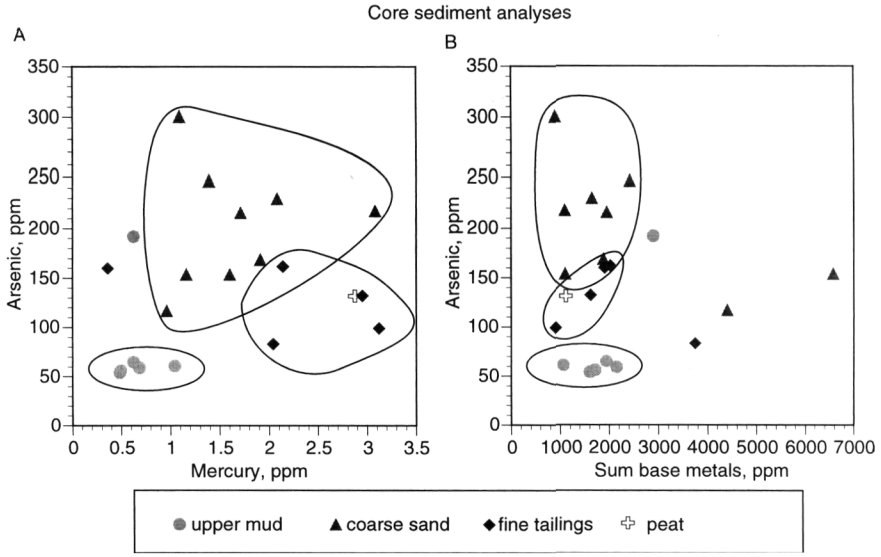

FIG. 8. Chemical trends in sediment cores (solid materials) of the Shawmut mill tailings (see Fig. 5). A. Arsenic concentration relative to mercury concentration. B. Arsenic concentration relative to base-metal concentrations. Chemical analyses are presented in Table 5.

base metals in the Shawmut tailings piles probably represent relict tailings from the Penn mine base-metal ores that were processed in the Shawmut mill.

The porewaters extracted from core sediment layers are calcium sulfate solutions (TDS = 80 to 2100 ppm), with pH values ranging from 3.7 to 7 (Fig. 9A). The lowest pH values are in the coarse sand and fine tailings layers, where gypsum is present. Mud porewaters are nearly neutral, as is the porewater in a peat layer within core 98-2. Tables 6 and 7 present selected chemical analyses of the porewaters. Arsenic and base metals in porewaters display trends that are somewhat different from their host sediments (Fig. 9). For example, whereas arsenic concentrations were lowest in the upper-mud solid materials, they are highest in the upper-mud porewaters where the range is 16 to 500 µg/L. Porewater extracted from a peat layer at the base of core 98-2 contained 180 µg/L arsenic. In porewaters of all of the other strata, as well as in the overlying lake water, arsenic concentrations are less than 10 µg/L except for three porewaters extracted from coarse sand samples with values of 20, 40, and 100 µg/L. The arsenic concentrations are correlated with pH; concentrations are highest in nearly neutral waters and decrease with more acidic pH values (Fig. 9A). Arsenic oxidation state was determined for porewaters extracted from cores 98-2, 98-3, and 98-4. All detected arsenic was As(III) in these samples except for the 98-3 core, in which 45% of the total arsenic was As(III),

The base-metal concentrations in the lake and porewaters, unlike in the sediments, are distinctive among the various strata (Fig. 9B). Base-metal concentrations in the coarse sand porewaters are highest but also the most variable, with concentrations between 0.04 and 950 mg/L for the sum of lead, zinc, copper, cadmium, cobalt, and nickel. The concentrations in the fine yellow-orange tailings porewaters are clustered between 7 and 36 mg/L, and the concentrations in the upper mud porewaters are all less than 1 mg/L. Concentrations in the overlying lake waters are lowest, less than 0.1 mg/L. In all of the core porewater samples, the major contribution to base metals is from zinc.

Lake waters

Waters in monomictic Don Pedro Reservoir (Fig. 2) are dilute calcium-magnesium carbonate solutions (TDS = 7 to 25 ppm). Figure 10 illustrates the development of temperature and pH stratification during the summer months; the profiles are not all from the same year, but they do represent the seasonal trends. In June, temperature stratification was already evident, whereas pH values were still relatively constant throughout the water column. Strati-

TABLE 5. Core Sediment Analyses

Sample	Description	[1]Na_2O wt%	K_2O wt%	CaO wt%	MgO wt%	Al_2O_3 wt%	SiO_2 wt%	Fe_2O_3 wt%	MnO wt%	P_2O_5 wt%	TiO_2 wt%	LOI wt%	Total wt%	[2]As ppm	Hg ppb	Cr ppm	Cd ppm	Co ppm	Cu ppm	Ni ppm	Pb ppm	Zn ppm
97-3 A	Mud	0.85	1.72	0.86	2.34	15.27	56.46	7.24	0.04	0.21	0.82	7.64	93.45	61	1050	98	3.5	14	238	72	180	568
97-3 B	Sand	0.93	1.43	0.45	1.66	8.54	63.82	4.87	<.01	0.11	0.46	2.58	84.85	154	1600	47	3.5	1	266	9	288	534
97-3 C	Fine yellow tailings	0.48	1.27	1.80	1.89	8.00	59.89	2.65	<.01	0.05	0.30	2.41	78.74	99	3120	14	0.5	<1	300	<1	350	256
97-6 A-1	Mud	0.96	1.41	0.71	1.87	12.13	63.69	6.30	0.04	0.15	0.66	5.31	93.24	59	690	76	8	11	445	56	150	1490
97-6 A-2	Clay	1.07	1.97	0.89	2.90	11.86	56.65	6.50	0.01	0.11	0.36	3.55	85.87	160	360	78	5	<1	487	12	420	986
97-6 B	Fine yellow tailings	0.66	2.04	2.47	3.25	13.03	53.12	3.56	0.01	0.07	0.29	4.37	82.87	132	2950	23	2	<1	402	4	620	592
97-6 C	Grey clay	0.73	2.26	2.25	3.60	12.66	55.22	2.91	0.02	0.05	0.33	3.27	83.30	83	2040	34	8	<1	1815	9	412	1500
97-8A	Mud	1.02	2.04	1.10	2.77	18.38	53.40	8.94	0.09	0.27	0.92	9.63	98.56	54	490	121	5.5	19	273	91	176	1050
97-8B	Sand	1.37	1.64	0.52	2.68	11.53	63.80	6.28	0.03	0.19	0.56	4.22	92.82	117	960	96	15	4	1025	46	350	2960
97-9 A	Mud	1.11	1.96	0.86	2.60	15.48	59.03	7.43	0.07	0.21	0.86	6.83	96.44	65	630	119	6.5	16	412	88	150	1280
97-9 B	Sand	1.57	1.56	0.77	2.75	10.12	62.92	6.61	0.03	0.13	0.46	3.43	90.35	154	1160	94	21	4	1535	33	520	4460
97-10A	Mud	1.30	2.06	1.11	2.56	16.68	53.81	8.57	0.07	0.24	0.86	8.39	96.65	56	500	126	5.5	18	406	83	220	990
97-10B(1)	Sand	1.03	2.15	0.80	3.26	12.46	51.20	9.08	0.02	0.11	0.39	6.99	87.49	169	1910	85	1	<1	445	14	1060	362
97-10 B(2)	Sand	0.99	2.14	0.76	3.29	12.75	52.50	9.22	0.02	0.13	0.39	6.27	88.46	216	1710	87	1.5	<1	446	13	1120	370
97-10 C	Fine yellow tailings	0.90	2.73	3.04	3.56	14.32	49.87	6.02	0.01	0.07	0.30	5.89	86.71	162	2140	55	1.5	<1	410	4	1200	406
98-2 B	Muddy sand													247	1390	107	7	6	671	36	258	1440
98-2 C	Yellow sand													230	2080	92	2	3	664	29	420	530
98-2 D	Brown sand													218	3080	54	0.5	1	309	11	522	250
98-2 F	Peat													133	2910	46	0.5	2	261	11	552	214
98-3	Mud													192	630	94	12.5	30	421	105	144	2200
98-4 B	Sand													301	1090	87	1.5	4	247	25	264	352

[1]Major-element compositions by XRF analyzed at Chemex Laboratories, Sparks, NV.
[2]Trace-element analyses by ICP-MS analyzed at Chemex Laboratories, Sparks, NV.

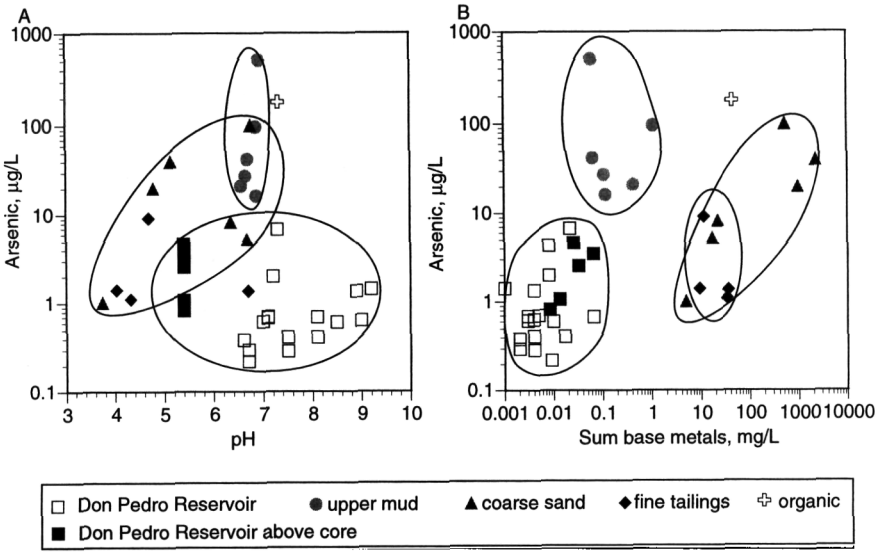

FIG. 9. Chemical trends in lake waters (Don Pedro Reservoir, Harvard open-pit mine lake) and sediment core porewaters of the Shawmut mill tailings. A. Arsenic concentration relative to pH. B. Arsenic concentration relative to base-metal concentrations. Chemical analyses are presented in Table 5.

fication was most highly developed in August for both temperature and pH. By October, surface waters had cooled, temperature stratification was diminishing, and pH near the lake surface had decreased.

The reservoir waters are relatively low in arsenic (Table 7). Surface waters near the Clio mine waste-rock pile at the reservoir shoreline consistently contained less than 1 µg/L arsenic, similar to background concentrations (0.2 to 0.4 µg/L) in the Tuolumne River approximately 7.5 km upstream (6 km northeast) of the Mother Lode belt. Arsenic concentrations in hypolimnion waters overlying the Shawmut tailings were 0.8 to 3.5 µg/L when cores were collected in October 1997, and 0.5 µg/L in June 1998 prior to the onset of summer stratification. The highest concentrations, 1.5 to 4.5 µg/L, were observed near the confluence of Woods Creek and Sullivan Creek (see Fig. 2); these concentrations are also far below the present U.S. Environmental Protection Agency maximum contaminant limit (EPA MCL, 50 µg/L). Base-metal concentrations in the reservoir waters also are significantly lower (less than 70 µg/L) than in the core porewaters (Fig. 9B); the dominant base-metal cation is zinc.

The Harvard mine pit lake, by contrast with Don Pedro Reservoir, receives most of its water from rain, associated surface runoff, and ground water, rather than from a sustained source of surface water. Dewatering during excavation of the Harvard open-pit mine (Jamestown mine) produced a hydrologic cone of depression that has been recovering toward the pre-mining groundwater configuration since mining ended in 1994. Rainfall is concentrated in the winter months. Each year since 1994, the area near the Harvard pit received 115 ± 30 cm of rain (http://cdec.water.ca.gov). Springs on the hanging wall introduce alkaline Ca-Mg-sulfate solutions (pH ~8.2; TDS ~3700 ppm; alkalinity ~160 mg/L reported as $CaCO_3$) with <10 µg/L arsenic. They produce tufas and efflorescences of gypsum, aragonite, and iron oxyhydroxides, and support an algal community. Groundwater sampled from a well into old underground workings northwest of the pit also is alkaline, and contains <10 µg/L arsenic (pH ~ 7.2).

At present, the pit lake consists of alkaline Ca-Mg-sulfate solutions (TDS ~ 1400 ppm; alkalinity ~ 110 mg/L reported as $CaCO_3$). Figure 11 shows daily rainfall for 1998 and pit-lake depth profiles of temperature, pH, dissolved oxygen, and filtered (0.45 µm) dissolved arsenic for five sampling events during the 1998 calendar year. Temperature profiles demonstrate that the Harvard mine pit lake is monomictic; minor upper-level thermal stratification develops in the summer and waters are well

TABLE 6. Shawmut Sediment Porewaters and Overlying Lake Waters[1]

Sample	Description	pH units	Na mg/L	K mg/l	Ca mg/l	Mg mg/l	Al mg/l	Si mg/l	As µg/l	Co µg/l	Ni µg/l	Cu µg/l	Zn µg/l	Cd µg/l	Pb mg/l	Sulfate mg/l
97ES-3-W	Water column	5.4	0.92	n.a.	3	1.0	0.007	0.58	2.5	0.5	0.7	1	30	<.1	0.5	7.1
97ES-3-A	Mud	6.7	1.80	n.a.	86	13.2	0.010	2.78	42.1	9.2	11.5	2	42	0.1	0.9	670
97ES-3-B	Sand	3.74	3.65	n.a.	317	35.7	0.862	5.94	1.0	125.8	244.4	671	3590	21.2	252.6	1700
97ES-3-C	Fine yellow tailings	4.03	3.75	n.a.	335	33.0	1.233	9.40	1.4	117.2	275.5	686	8021	27.4	153.4	n.a.
97ES-6-W	Water column	5.4	0.95	n.a.	3	0.9	0.005	0.60	1.1	0.3	0.7	1	11	0.0	0.4	2.1
97ES-6-A1	Mud	6.57	1.97	n.a.	64	16.8	0.005	3.11	21.0	10.4	13.4	1	411	0.1	0.5	580
97ES-6-A2	Clay	4.69	3.93	n.a.	306	55.3	0.082	9.10	9.2	57.9	138.3	22	11298	40.8	14.1	1600
97ES-6-B	Fine yellow tailings	4.32	5.83	n.a.	310	102.2	0.600	7.58	1.1	96.5	291.9	188	32526	205.7	413.1	n.a.
97ES-6-C	Grey clay	6.7	4.33	n.a.	315	97.2	0.730	8.46	1.4	104.1	295.0	943	33896	200.0	391.0	1500
97ES-8-WW	Water column[2]	5.4	1.05	n.a.	4	1.2	0.078	0.62	3.5	0.8	1.3	2	57	0.1	2.7	NA
97ES-8-A	Mud	6.66	1.84	n.a.	36	11.5	0.004	2.03	27.3	5.1	4.2	0	101	0.0	0.1	210
97ES-8-B	Sand	6.35	4.41	n.a.	153	38.9	0.020	1.69	8.3	96.2	145.1	10	21892	116.2	4.3	870
97ES-9-W	Water column	5.4	0.93	n.a.	3	1.2	0.017	0.66	4.7	0.6	0.9	1	23	0.0	0.7	6.8
97ES-9-A	Mud	6.88	2.36	n.a.	56	14.8	0.003	2.57	96.0	16.0	14.8	2	1106	0.2	1.8	250
97ES-9-B	Sand	6.68	5.23	n.a.	190	38.6	0.031	1.60	5.3	98.3	119.6	148	16421	419.1	9.5	930
97ES-10-W	Water column	5.4	0.89	n.a.	2	0.8	0.004	0.57	0.8	0.2	0.6	1	7	0.0	0.1	2.1
97ES-10-A	Mud	6.88	1.57	n.a.	39	7.1	0.022	2.30	16.3	4.0	4.4	1	109	0.1	0.6	200
97ES-10-B	Sand	4.31	3.42	n.a.	302	24.1	0.474	7.02	0.0	53.4	76.0	393	3076	9.9	132.5	270
97ES-10-C	Fine yellow tailings	3.98	4.34	n.a.	327	26.1	1.507	6.07	0.0	27.9	74.7	1121	5910	37.8	388.2	1500
*98ES-2	Water column	7.59	3.80	1 .00	10.35	4.37	0.009	n.a.	<1	0.1	1.0	3	9	<0.1	<2	9.8
*98ES-28	Muddy sand	4.78	4.5	6	274	37	0.030	n.a.	20	27.8	36.0	4	885	6	<20	100
*98ES-2C	Yellow sand	5.13	3	4.5	491	11.65	0.120	n.a.	40	9	40.0	148	1890	9	100	140
*98ES-2D	Brown sand	6.76	3.75	5	567.5	4.875	0.250	n.a.	100	3.5	15.0	35	475	<2.5	<50	61
*98ES-2F	Black organic	7.32	2.5	4.5	561	5.39	0.100	n.a.	180	1.8	6.0	2	35	<1	<20	140
*98ES-3PW	Mud	6.94	5.15	3.90	53.4	13.90	0.034	n.a	508.0	5.0	2.8	5	46	0.1	4.0	<0.2
*98ES-4B	Sand	4.77	3.5	2.5	17	2.9	0.050	n.a.	<10	7.2	12.0	77	280	2	<20	8.8

[1]All samples were analyzed by ICP-MS at Actlabs Inc. (Colorado) unless marked with an asterisk (*); marked samples were analyzed by ICP-MS at Chemex Laboratories (Nevada). Sulfate concentrations were analyzed by ion chromatography at U.S. Geological Survey Water Resources Labs (Florida); n.a. = not analyzed; n.d. = below detection limit.
[2]Unfiltered.

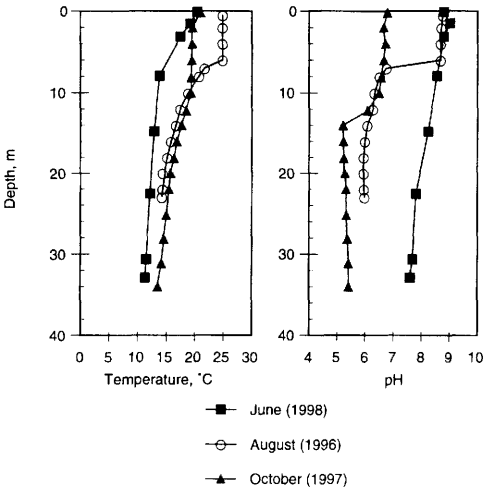

FIG. 10. Temperature and pH profiles of Don Pedro Reservoir near the Shawmut mine, illustrating stratification during early, mid-, and late summer. Data collected using a Hydrolab™ Minisonde Multiprobe.

mixed in winter. The lake pH, buffered by carbonate minerals in the wall rock, remains nearly neutral throughout the year and exhibits only slight summer stratification. This contrasts with Don Pedro Reservoir waters, which vary vertically by nearly four pH units during summer stratification (Fig. 10). Dissolved oxygen is low in the deep waters (>200 feet) of the pit lake throughout the year, at times reaching values near zero but never becoming completely anoxic except at the very bottom (where the measuring device may be in sediment). Oxygen depletion extends upward to middle depths during late summer, showing undersaturation at depths below 100 to 150 feet in October and November prior to lake turnover, which occurred between our November 11 and December 13 sampling events.

By contrast with waters of Don Pedro Reservoir, arsenic concentrations in the Harvard mine-pit lake are well above the EPA MCL at 800 to 1000 μg/L. Base-metal concentrations in the Harvard mine-pit lake water column (80 to 150 μg/L) are also significantly higher than in Don Pedro Reservoir waters (less than 70 μg/L). In both the core porewaters and Don Pedro Reservoir waters, the greatest contribution to base metals is from zinc, whereas in the Harvard mine-pit lake, the greatest contribution is from nickel, reflecting the composition of ultramafic rocks in the footwall.

Figure 11 shows that dissolved arsenic (operationally defined as passing through a 0.45 μm filter) was of relatively constant concentration throughout the pit-lake water column during the winter mixis (March, June), but was redistributed during the summer. By the end of the summer dry period (October), the highest concentrations were at intermediate depth. At this time, arsenic concentrations in the shallow waters, where the pit has its largest diameter, were slightly lower (785 μg/L at surface and at 75 feet) than their June values (June: 785 μg/L at surface, 840 μg/L at 75 feet). Calculating the total mass of arsenic in the pit indicates that there was redistribution but little net flux between June and October. However, an overall arsenic increase occurred with onset of winter rains as seen in the marked change between October 23 and November 11. Arsenic concentration in the upper lake waters increased by approximately 200 μg/L at this time, contributing significantly to the total mass of arsenic in the lake. By December 13, dissolved arsenic concentration throughout the lake had decreased, although not to values as low as the previous spring. Possible causes for the seasonal changes in arsenic concentration and distribution are addressed in the discussion.

Discussion

Arsenic in the surface and aquatic environments described above originated from arsenian pyrite formed during gold mineralization in the Mother Lode. Diverse geochemical and biogeochemical pathways govern its distribution and transport as it moves from its host lithologic environments into weathering and aquatic environments (Fig. 12). Pyrite exposed to atmospheric oxygen and rainwater on outcrop surfaces, joints and cracks, and on mine waste-rock surfaces, oxidizes to produce acidic solutions that accelerate silicate and carbonate weathering. Since arsenic occurs as solid solution in pyrite, the kinetics of arsenic release are determined by the pyrite oxidation rate. At ambient temperatures and pressures, this rate is a sensitive function of dissolved oxygen, ferric iron content, and pH (McKibben and Barnes, 1986; Moses and Herman, 1991; Williamson and Rimstidt, 1994). Ferric iron is particularly important as an oxidant in acidic environments (see also Moses et al., 1987; Brown and Jurinak, 1989; Stumm and Morgan, 1996). Production of ferric iron from ferrous iron is catalyzed by numerous microbes, such as the aerobic, acido-

TABLE 7. Don Pedro Reservoir Waters[1]

Sample	Month, location, depth	pH units	Na mg/l	Ca mg/l	Mg mg/l	Al mg/l	Si mg/l	As µg/l	Co µg/l	Ni µg/l	Cu µg/l	Zn µg/l	Cd µg/Al	Pb µg/l
96DP-095	November mixis (Shawmut, 5 m)	7.1	1.73	3.9	2.0	0.003	0.39	0.73	0.05	0.8	2.73	1.8	0.01	0.02
96DP-096	November mixis (Shawmut, 0.2 m)	7.1	1.98	5.6	2.3	0.023	0.37	0.71	0.11	0.9	1.75	63.3	0.03	0.12
96DP-097	November mixis (Shawmut, 12 m)	7.0	1.82	4.3	2.1	0.002	0.43	0.64	0.05	0.7	1.53	1.2	n.d.	<.002
96DP-100	November mixis (Clio, 0.3 m)	7.5	1.35	3.1	1.4	0.004	0.37	0.43	0.06	1.3	1.78	1.1	n.d.	0.01
96DP-101	November mixis (Clio, 9 m)	7.5	1.33	2.8	1.4	0.003	0.32	0.30	0.03	0.7	1.11	2.2	n.d.	<.002
97DP-150 A	August epilimnion (18-mile mark, 0.3 m)	8.1	112	2.4	1.2	0.016	0.76	0.43	0.03	1.0	2.24	12.5	0.06	1.11
97DP-150 B	August hypolimnion (18-mile mark, 11 m)	6.7	0.82	2.0	0.5	0.012	0.51	0.23	0.02	0.6	1.15	7.3	0.03	0.30
97DP-151 A	August epilimnion (Clio, 0.3 m)	8.1	1.39	3.2	1.4	0.013	0.88	0.72	0.03	0.9	0.48	1.7	n.d.	n.d.
97DP-151 B	August hypolimnion (Clio, 14 m)	6.7	0.78	2.4	0.6	0.030	0.54	0.31	0.06	0.5	0.17	0.9	n.d.	n.d.
97DP-152 A	August epilimnion (Shawmut, 0.3 m)	9.0	1.41	2.6	1.4	0.018	1.01	0.66	0.02	0.6	0.36	3.4	n.d	0.11
97DP-152 B	August hypolimnion (Shawmut, 21 m)	6.6	1.08	2.6	0.7	0.010	0.78	0.40	0.02	0.4	0.23	1.6	n.d.	n.d.
97DP-153 A	August epilimnion (Woods Crk., 0.3 m)	9.2	2.53	4.9	2.8	0.015	1.33	1.47	0.06	0.67	0.50	n.d.	n.d.	n.d.
97DP-153 B	August hypolimnion (Woods Crk., 4 m)	7.2	2.02	4.8	2.3	0.007	1.28	2.06	0.16	1.03	0.33	6.5	0.01	0.19

[1]All samples were analyzed by ICP-MS at Actlabs, Inc. (Colorado); see Note 1, Table 6 for symbols and abbreviations.

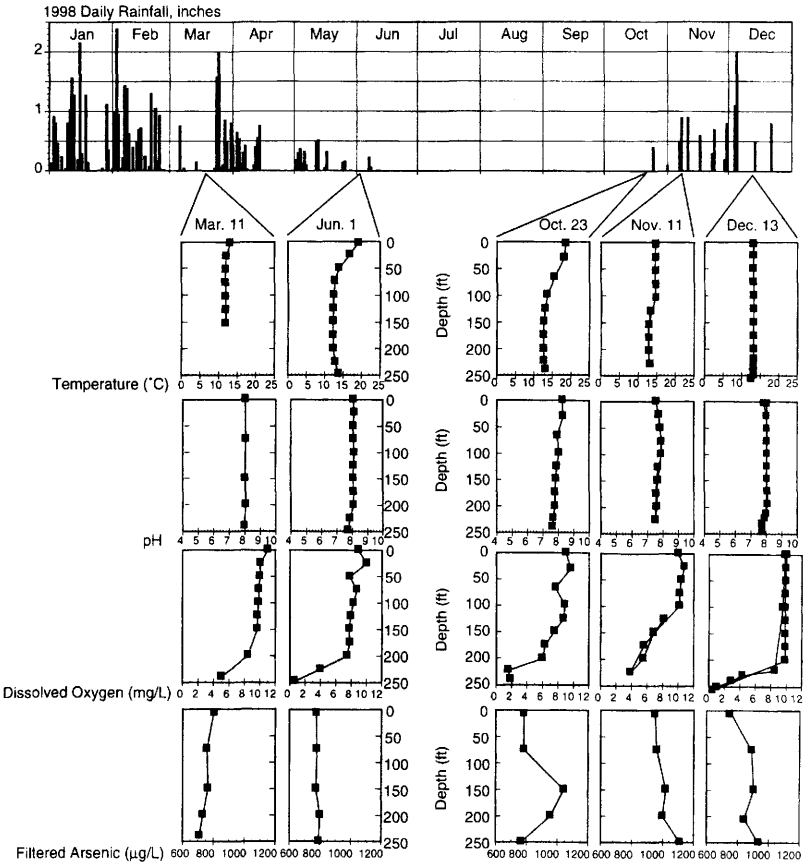

FIG. 11. Daily rainfall near the Harvard mine-pit lake (Sonora station, California Dept. of Forestry) and temperature, pH, dissolved oxygen, and dissolved (<0.45 pm) arsenic concentration profiles in the pit lake during five sampling events in 1998 (see text).

philic bacterium *Thiobacillus ferrooxidans* (Singer and Stumm, 1970). The ferric iron accepts electrons from the disulfide in pyrite, autocatalyzing pyrite oxidation (Eggleston et al., 1996). *T. ferrooxidans* is most active near 30°C and at pH near 2–3 (Singer and Stumm, 1970; Jaynes et al., 1984; Collinet and Morin, 1990). In alkaline solutions, such as the Harvard mine-pit lake waters, oxidation rates of fresh pyrite surfaces are increased by the complexation of Fe^{2+} [aquo-complex] with bicarbonate ions (Evangelou et al., 1998), but pyrite surfaces are rapidly passivated by precipitation of iron oxyhydroxide coatings (Moses and Herman, 1991; Nesbitt et al., 1995; Al et al., 1997; Nicholson et al., 1988, 1990).

The clustered substitution of arsenic for sulfur in pyrite, as we have determined from samples of the Clio mine (Savage et al., 2000), also may be responsible for accelerating oxidation and dissolution of arsenian pyrite relative to pyrite. Arsenian pyrite is more reactive than arsenic-poor pyrite (Fleet et al., 1993; Huggins et al., 1997). In samples of the Clio mine, arsenian pyrite grains have thicker oxidized rinds than pyrite with low arsenic (Tingle et al., 1996). The enhanced reaction rate might be expected from increased electrical and ionic conductivity of the pyrite caused by carriers created by the As-for-S substitution (Evangelou and Zhang, 1995). Arsenic replacing sulfur in pyrite creates p-type semiconducting regions that trap electrons (Moller and Kersten, 1994). Such regions can act as electron donors for the reduction of metal ions or complexes approaching the pyrite/aqueous solution interface, thereby influencing surface reactivity.

Pyrite oxidation in the weathering environment produces iron sulfate and iron oxyhydroxide phases

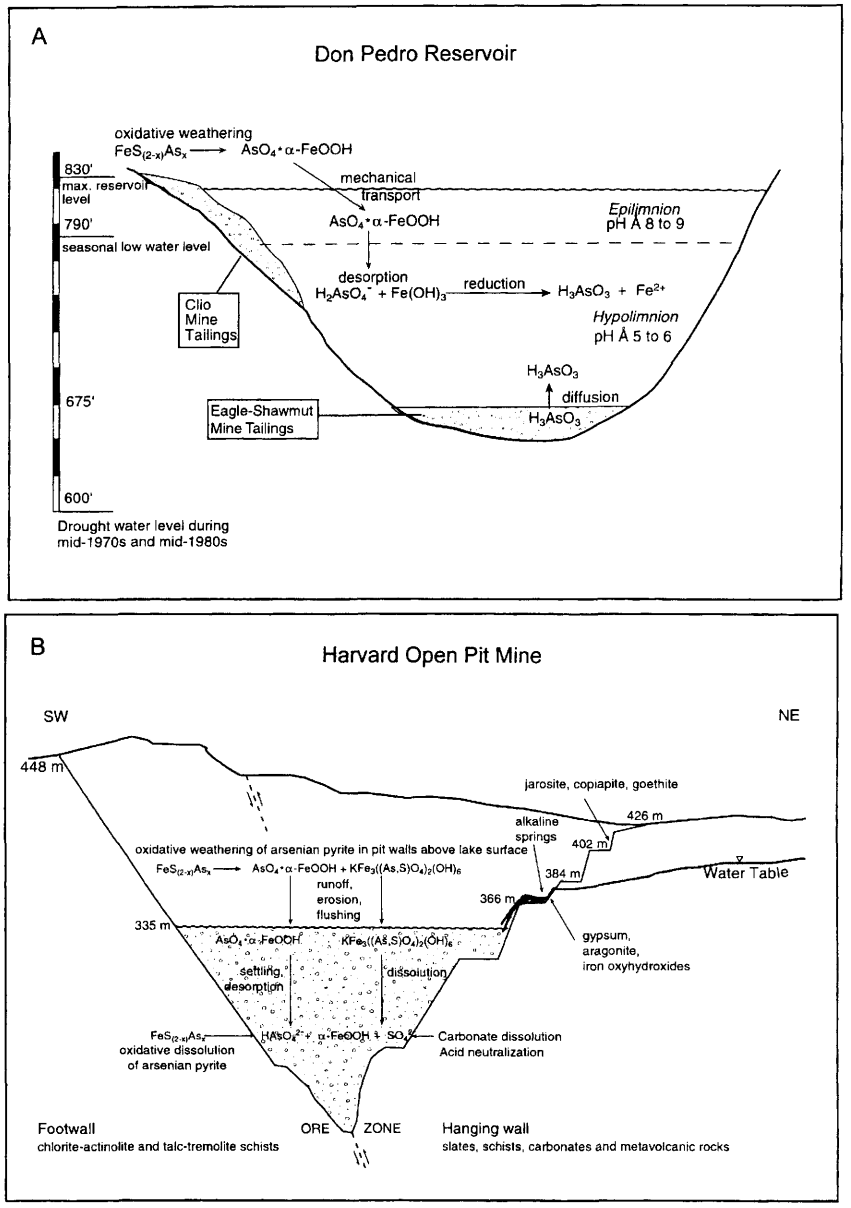

FIG. 12. A. Schematic cross section of Don Pedro Reservoir showing simplified hydrogeochemical pathways of arsenic. Seasonal rainfall erodes or dissolves arsenic-bearing weathering products of arsenian pyrite, flushing them into the reservoir. Arsenate sorbed (or coprecipitated) on goethite desorbs under alkaline conditions. Iron and arsenic in mill tailings may be remobilized upon reductive dissolution. Summer thermocline indicated by dashed line. B. Schematic cross section of the Harvard open-pit mine lake illustrating arsenic pathways. Here dissolution of arsenic-bearing efflorescent salts introduces arsenic into the pit lake. Lake waters buffered at pH 7 to 9 throughout the year by carbonate minerals in the pit-wall rocks limit arsenic sorption onto particulate materials.

including jarosite, goethite, and copiapite, as well as others not yet observed in our study area, such as rozenite and melanterite (Jambor, 1994). Carlson et al. (1992) found that bacterially mediated oxidation of arsenian pyrite (11% arsenic, much higher than in pyrite of the southern Mother Lode Gold District)

produced mixtures of scorodite with jarosite. Scorodite has not been observed by the authors in any of the locations in this study, although it was reported in the Jamestown mining district by Goudey (1947).

The geochemistry of arsenic in weathering and aquatic environments involves oxidation-reduction, ligand exchange, precipitation/dissolution, and sorption/desorption (Ferguson and Gavis, 1972). Arsenic released from arsenian pyrite (or other minerals) in the weathering environment may adsorb onto or coprecipitate with secondary phases and colloids (Fig. 12). In our study area, we observe three dominant secondary minerals with which arsenic is associated on rock surfaces. Weathering products forming fine-grained friable crusts on outcrops of the Harvard pit above the elevation of alkaline springs (Fig. 4B) consist primarily of mixtures of jarosite, copiapite, and goethite as well as other iron oxyhydroxides. On waste rock of the Clio mine, goethite is the major secondary mineral hosting arsenic; on outcrops near the Harriman mine, both goethite and jarosite are present and are associated with arsenic. Which minerals form depends on the mineralogic environment in the immediate vicinity of the weathering pyrite. Goethite primarily forms where high-pH buffering minerals such as calcite, magnesite, or albite are abundant in the outcrops and tailings, whereas jarosite and copiapite form in environments where the rock locally has minimal pH-buffering capacity. It is not uncommon in sulfide weathering environments to observe a "bull's eye" pattern on weathering surfaces with copiapite at the center, surrounded by jarosite and goethite (Sanches Montero et al., 1999). This pattern is observed on the Harvard mine pit wall, with copiapite occurring where a low-angle joint meets the rock face; jarosite and goethite surround the copiapite on the rock face within 10 to 30 cm above and below the joint.

Arsenic is transported into aqueous environments such as Don Pedro Reservoir and the Harvard mine-pit lake by erosion and/or dissolution of arsenic-bearing secondary minerals (Fig 12). The mode of arsenic association as well as differences in mineral solubilities have important consequences for release of arsenic into the aquatic environment. Copiapite is an efflorescent mineral with very high solubility; early winter storms dissolve copiapite from rock surfaces and transport its constituents into surface runoff (Bayless and Olyphant, 1993). Jarosite is far less soluble but is stable only under acidic conditions (Baron and Palmer, 1996); therefore, it too dissolves, given sufficient time and buffering capacity to keep pH near-neutral or above, releasing associated arsenic to surface or ground waters. Arsenic associated with goethite desorbs at neutral to alkaline pH, although the mineral substrate is stable under these conditions (see Brookins, 1988). Arsenic attenuation by these minerals during pyrite oxidation must be considered as temporary, depending on seasonal and longer-scale weather patterns such as El Niño/La Niña.

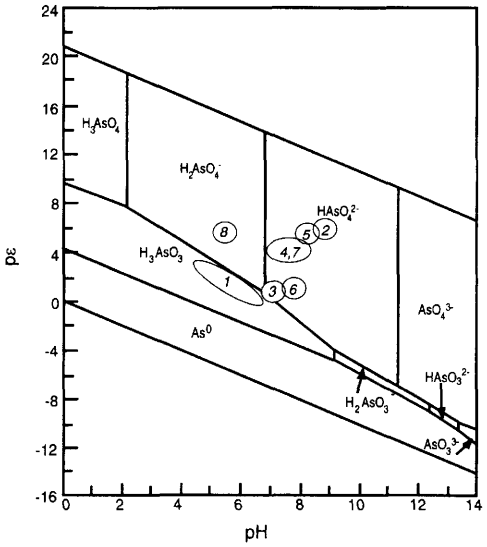

FIG. 13. Approximate pε and pH of waters from Don Pedro Reservoir, Shawmut mill tailings porewaters, and the Harvard mine-pit lake superimposed on a predominance diagram for the As-H_2-O_2 system as a function of pH and pε at 25°C, 1 bar. Arsenic speciation (solid phases not shown) from thermodynamic data in Bowell et al. (1994), Cherry et al. (1979), Pokrovski (1996), and Hem (1977). Symbols: 1 = Shawmut core porewaters; 2 = Don Pedro Reservoir epilimnion; 3 = Don Pedro Reservoir hypolimnion; 4 = Don Pedro mixis; 5 = Harvard pit lake epilimnion; 6 = Harvard pit lake hypolimnion; 7 = Harvard pit lake mixis; 8 = rainwater.

Arsenic speciation in lakes and their sediments is affected by lake stratification and turnover (e.g., Aggett and O'Brien, 1985; Seyler and Martin, 1989; Kuhn and Sigg, 1993) because of the accompanying variations in pH and redox potential (Cherry et al., 1979; Thanabalasingam and Pickering, 1986). Arsenic hydrolyzes to form weak acids and commonly displays either of two redox states—As(III) or As(V)—in waters. Figure 13 illustrates that singly protonated As(V) [$HAsO_4^{2-}$] is thermodynamically favored in oxidized, neutral pH waters such as the

lake mixis and epilimnion of both the Harvard mine-pit lake and Don Pedro Reservoir (see Figs. 10 and 11), and while fully protonated As(III) [H_3AsO_3] is favored in reduced environments, such as the porewaters in submerged mill tailings of the Shawmut mine (Fig. 5). As for many elements with multiple redox conditions, toxicity differs between the two valences, with As(III) having more adverse effects on aquatic life (Eisler, 1994, and references therein). The oxidation rate of As(III) to As(V) is increased by the presence of *T. ferrooxidans* because of increased production of the oxidant Fe^{3+} (Mandl and Vyskovsky, 1994). Reduction of arsenate to arsenite can also be bacterially mediated (Stolz and Oremland, 1999). Methylated organoarsenical species also are important in some environments—e.g. aerobic soil porewaters (Bowell et al., 1994), estuaries (Anderson and Bruland, 1991; Sanders et al. 1994 and references therein), and some lake surface waters (Anderson and Bruland, 1991). Organoarsenical species were not determined in waters of this study.

Particulate materials exert significant control on arsenic mobility in aqueous environments by providing surfaces for sorption (see also Smith et al., 1992; Brown et al., 1999). Numerous studies show that arsenic demonstrates typical anion sorption behavior in that it adsorbs most strongly in acidic solutions. EXAFS analysis suggests that both arsenate (Waychunas et al., 1993) and arsenite (Manning et al., 1998) form bidentate surface complexes on goethite and ferrihydrite. The extent of arsenic sorption is influenced by the presence of competing anions such as sulfate (Wilkie and Hering, 1996) and phosphate (Manning and Goldberg, 1996), and the physico-chemical properties of the mineral surface (Frost and Griffin 1977; Manning and Goldberg, 1996).

Iron oxyhydroxides, as well as other particulate materials that may contain arsenic either as a constituent or as a sorbate, are introduced into lake bottom sediments by settling (Chapman et al., 1983; Crecelius, 1975). Abiotic and biotic reaction pathways (Cullen and Reimer, 1989; Belzile and Tessier, 1990; Dowdle et al., 1996) lead to iron and arsenic reduction following burial, causing arsenite to be released to porewaters. Sorbed arsenate also can be released by biotic reduction of iron oxyhydroxide phases (Cummings et al., 1999). Concentrations of arsenic in sediment porewaters have been found to exceed those in overlying lake waters at mine-impacted sites by a factor of up to 60 (Peterson and Carpenter, 1986; Azcue et al., 1994). An example of this is illustrated by the data in Figure 9. Porewaters of the upper mud layer overlying the Shawmut tailings contain ~20 times the arsenic concentrations in lake waters immediately above the cores, and up to 150 times the concentrations in lake waters away from the tailings piles (Fig. 9; Tables 6 and 7). Here the origin of the arsenic is primarily in the sediments (mill tailings) themselves, and it is not clear to what extent settling of arsenic-bearing particles from the water column contributes to the porewater arsenic concentrations. In anoxic waters (i.e., summer hypolimnion of stratified lakes), concentration gradients between sediments and overlying waters drive upward diffusion of arsenic—both As(III) and As(V)—into the lake water column, a process that is accelerated by sediment compaction (Aggett and O'Brien, 1985; Brannon and Patrick, 1987; Azcue et al., 1994).

Liberation of arsenic in flooded sediments may be mediated by microbial iron reduction—for example by *Shewanella alga* (Cummings et al., 1999). Hence arsenic attenuated in sediments may be remobilized, and dispersed throughout the lake during the winter mixis. Because Don Pedro Reservoir has a large and variable volumetric influx of water from the Tuolumne River watershed in the high Sierra, especially during the late spring when snowmelt runoff peaks, it is difficult to quantitatively estimate the seasonal fluxes of arsenic from the sources in the study area. The mixis concentrations we measured in Don Pedro Reservoir are not significantly greater than concentrations of either the epilimnion or the hypolimnion during summer stratification. Epilimnion concentrations slightly exceed hypolimnion concentrations except immediately above the tailings piles and at the Woods Creek site (Table 7). This suggests that the source of arsenic in the summer epilimnion is influx from arsenic-bearing sediments as a result of shoreline erosion, such as friable weathering crusts of the Clio mine waste rock that are washed into the reservoir. Shoreline erosion increases during the summer months when recreational boaters create significant wake waves.

The high arsenic concentration relative to base-metals concentration in the Harvard mine-pit lake is consistent with pit-lake chemistry models for other alkaline open-pit mine lakes (Davis and Eary, 1997; Eary 1999), in which concentrations of oxyanions such as arsenic and selenium are typically elevated and cationic metals are low. This is in contrast with pit lakes in acid-dominated systems such as mas-

sive-sulfide deposits (as well as acid mine drainage waters), where dissolved metals can be extremely elevated. For example, [Cd + Cu + Zn] concentration at the Berkeley pit was up to 600 mg/L (Davis and Ashenberg, 1989) and [Cd + Co + Cu + Ni + Pb + Zn] can comprise up to 10,000 mg/L of acid-mine-drainage waters (Plumlee et al., 1994).

The concentration and distribution of arsenic in the Harvard mine-pit lake vary seasonally and with depth, as shown in Figure 11. The major change in mass distribution occurs during the summer stratification, demonstrated by the arsenic profiles in June and October 1998. Arsenic concentration in October was highest beneath the thermocline. The mechanism of redistribution is not yet well understood. Possibilities are: release from sediments and colloids by desorption or reductive dissolution of the particles under the redox conditions present at intermediate depths; introduction of arsenic by groundwater; or microbial activity at intermediate depths. None of these explanations is entirely satisfactory, however. Unfiltered and filtered samples from the June sampling event do not show significant differences in arsenic concentration, indicating that little arsenic was adsorbed to particulate material. There is also very little sediment present on the sides and bottom of the pit to account for arsenic flux. Introduction by groundwater is problematic because we do not observe a net mass increase, but rather a mass redistribution during this time period. Finally, there has been no study of microbiological communities in the pit lake to date.

Explanations for the mass changes between October and November in the Harvard mine-pit lake are less ambiguous. The major increase in concentration and total mass of arsenic in the pit lake occurred after the first winter storm; concentration subsequently decreased with continued rains throughout November and early December. Arsenic concentrations increased both in the upper portion of the pit lake, and at depth (Fig. 11). Because of the short time between sampling events (three weeks), during which the mass increase occurred, together with the observation of arsenic-bearing soluble salts present on the pit walls that developed during the summer months, we suggest that rain and storm runoff eroded and dissolved the salts both on the pit walls and in joints and cracks. The resulting solutions, which contain arsenic and sulfate, are introduced to the pit lake from runoff (influencing the surface waters) and groundwater (causing the concentration increase at the bottom of the lake). The subsequent concentration decrease, especially in the pit surface waters (Fig. 11, December) can be explained by dilution from additional rain and runoff after soluble salts on rock surfaces had been depleted. The presence of relatively higher arsenic concentration at the pit lake bottom through December is probably a consequence of the longer residence time of groundwater relative to storm runoff.

Conclusions

Arsenic concentration, speciation, and distribution in the Sierra Nevada foothills depend on many factors including the lithologic sources of arsenic, climatic influences on weathering of host minerals, and geochemical characteristics of waters with which source and secondary minerals react. This study has examined some of the influences on arsenic geochemistry in the southern Mother Lode Gold District of California in a water reservoir, open-pit mine lake, and submerged gold-mine mill tailings. Oxidation of arsenian pyrite to goethite, jarosite, and copiapite causes temporary attenuation of arsenic during summer when these secondary minerals accumulate; subsequent rapid dissemination of arsenic into the aqueous environment is caused by annual winter storms. As the population of the Mother Lode area grows, it becomes increasingly important to consider these effects during planning and development of land and groundwater resources.

Acknowledgments

This communication benefited from discussions with and review by Andrea Foster of the U.S. Geological Survey Mineral Resources Program. We would like to thank Michael Hunerlach and Charles N. Alpers of the U.S. Geological Survey Water Resources Program for assistance in collecting and processing sediment cores. Michael Parsons and Clara Chan also provided lab support during core collection and processing. We thank Gary Wilson for access to the Harvard mine pit, and Ed Coogan and Ross Grunwald for helpful discussions on the pit-wall outcrops. We also appreciate many discussions with Peggy O'Day and Glenn Waychunas. Our friend and colleague the late Tracy Tingle was involved in the earliest stages of this project and collected the data for the microprobe maps of pyrite arsenic concentration. Funding from the Mineral Resources Program of the USGS, the Stanford University Office

of the Dean of Research Grant 127P047 (to DKB), the U.S. Environmental Protection Agency "STAR" fellowship program and the Stanford School of Earth Science McGee and Shell Funds (to KSS), and NSF Grant EAR-9902859 (to DKB) is gratefully acknowledged. This paper represents a portion of the senior author's Ph.D. thesis at Stanford University.

REFERENCES

Aggett, J., and O'Brien, G. A., 1985, Detailed model for the mobility of arsenic in lacustrine sediments based on measurements in Lake Ohakuri: Environ. Sci. Technol., v. 19, p. 231–238.

Al, T. A., Blowes, D. W., Martin, C. J.., Cabri L. J., and Jambor, J. L.. 1997, Aqueous geochemistry and analysis of pyrite surfaces in sulfide-rich mine tailings: Geochim. et Cosmochim. Acta, v. 61, p. 2353–2366.

Allgood, G. M., 1990, Geology and operations at the Jamestown Mine, Sonora Mining Corporation, California, *in* Landefeld, L. A., and Snow, G. G., eds., Yosemite and the Mother Lode Gold Belt. Los Angeles: Amer. Assoc. Petrol. Geol., Pacific Sect., AAPG, p. 147–154.

Allgood, G. M., Allgood, R. W., and Preadenas, J., 1987, Gold occurrences in Tuolumne County, California: Mineralogical Record, v. 18, p. 41–64.

Anderson, L. C. D., and Bruland, K. W., 1991, Biogeochemistry of arsenic in natural waters: The importance of methylated species: Envt. Sci. Technol., v. 25, p. 420–427.

Ashley, R. P., and Ziarkowski, D. V., 1999, Arsenic in waters affected by mill tailings at the Lava Cap Mine, Nevada County, California: Geol. Soc. Amer. Abs. Prog., v. 31, no. 6, p. A35.

Azcue, J. M., Nriagu, J. O., and Schiff, S., 1994, Role of sediment porewater in the cycling of arsenic in a mine-polluted lake: Environ. Int., v. 20, p. 517–527.

Baron, D., and Palmer, C. D., 1996, Solubility of jarosite at 4–35°C: Geochim. et Cosmochim. Acta, v. 60, p. 185–195.

Bayless, E. R., and Olyphant, G. A., 1993, Acid-generating salts and their relationship to the chemistry of groundwater and storm runoff at an abandoned mine site in southwestern Indiana, U.S.A.: Jour. Contam. Hydrol., v. 12, p. 313–28.

Belzile, N., and Tessier, A., 1990, Interactions between arsenic and iron oxyhydroxides in lacustrine sediments: Geochim. et Cosmochim. Acta, v. 54, p. 103–109.

Bohlke, J. K., and Kistler, R. W., 1986, Rb-Sr, K-Ar, and stable isotope evidence for the ages and sources of fluid components of gold-bearing quartz veins in the northern Sierra Nevada foothills metamorphic belt, California: Econ. Geol., v. 81, p. 296–322.

Bowell, R. J., Morley, N. H., and Din, V. K., 1994, Arsenic speciation in soil porewaters from the Ashanti Mine, Ghana: Appl. Geochem., v. 9, p. 15–22.

Brannon, J. M., and Patrick, W. H., Jr., 1987, Fixation, transformation, and mobilization of arsenic in sediments: Environ. Sci. Technol., v. 21, p. 450–459.

Brookins, D. G., 1988, Eh-pH diagrams for geochemistry: Berlin, Springer-Verlag.

Brown, A. D., and Jurinak, J. J., 1989, Mechanism of pyrite oxidation in aqueous mixtures: Jour. Environ. Quality, v. 18, p. 545–550.

Brown, G. E., Jr., Foster, A. L., and Ostergren, J. D., 1999, Mineral surfaces and bioavailability of heavy metals: A molecular-scale perspective: Proc. Nat. Acad. Sci. U.S.A., v. 96, p. 3388–3395.

California Regional Water Quality Control Board, 1999, Draft minutes, 427th Regular Meeting California Regional Water Quality Control Board, Central Valley Region. Sacramento, CA: State of California.

Carlson, L., Lindstroem, E. B., Hallberg, K. B., and Touvinen, O. H., 1992, Solid-phase products of bacterial oxidation of arsenical pyrite: Appl. Environ. Microbiol., v. 58, 1046–1049.

Chaffee, M. A., and Sutley, S. J., 1994, Analytical results, mineralogical data, and distributions of anomalies for elements and minerals in three mother lode-type gold deposits, Hodson mining district, Calaveras County, California: U. S. Geol. Surv. Open File Report 94640A.

Chapman, B. M., Jones, D. R., and Jung, R. F., 1983, Processes controlling metal ion attenuation in acid mine drainage streams: Geochim. et Cosmochim. Acta, v. 47, p. 1957–1973.

Cherry, J. A., Shaikh, A. U., Tallman, L. E., and Nicholson, R. V., 1979, Arsenic species as an indicator of redox conditions in groundwater: Jour. Hydrol., v. 43, p. 373–392.

Clark, W. B., 1970, Gold Districts of California: Sacramento, CA, California Division of Mines and Geology.

Collinet, M.-N., and Morin, D., 1990, Characterization of arsenopyrite oxidizing *Thiobacillus*. Tolerance to arsenite, arsenate, ferrous, and ferric iron: Antonie van Leeuwenhoek Int. Jour. General Molec. Microbiol., v. 57, p. 237–244.

Crecelius, E. A., 1975, The geochemical cycle of arsenic in Lake Washington and its relation to other elements: Limnol. Oceanog., v. 20, p. 441–451.

Cullen, W. R., and Reimer, K. J., 1989, Arsenic speciation in the environment: Chem. Rev., v. 89, p. 713–764.

Cummings, D. E., Caccavo, F., Fendorf, S., and Rosenzweig, R. F., 1999, Arsenic mobilization by the dissimilatory Fe(III)-reducing bacterium *Shewanella alga* BrY: Environ Sci. Technol., v. 33, p. 723–729.

Davis, A., and Ashenberg, D., 1989, The. aqueous geochemistry of the Berkeley Pit, Butte, Montana, U.S.A.: Appl. Geochem., v. 4, no. 1, p. 23–36.

Davis, A., and Eary, L. E., 1997, Pit lake water quality in the western United States: An analysis of chemogenetic trends: Min. Eng.. v. 49, no. 6, p. 98–102.

Dohms, P. H., Hoagland, R. D., and Allgood, G. M., 1985, Geology of the Jamestown Mine area, Mother Lode Gold Belt, Tuolumne County, California, *in* Slavik, G., ed., Geologic cross section across the southern Mother Lode Belt: Harvard mine, Royal-Mountain King mine, Gold Cliff mine: Reno, NV, Geol. Soc. Nevada.

Donovan, J. J., and Tingle, T. N., 1996, An improved mean atomic number background correction for quantitative microanalysis: Jour. Microsc. Soc. Amer., v. 2, p. 1–7.

Dowdle, P. R., Laverman, A. M., and Oremland, R. S., 1996, Bacterial dissimilatory reduction of Arsenic(V) to Arsenic(III) in anoxic sediments: Appl. Environ. Microbiol., v. 62, p.1664–1669.

Dutrizac, J. E., and Jambor, J. L., 1987, The behavior of arsenic during jarosite precipitation: Arsenic precipitation at 97° from sulfate or chloride media: Can. Metall. Quart., v. 26, no. 2, p. 91–101.

Dutrizac, J. E., Jambor, J. L., and Chen, T. T., 1987, The behavior of arsenic during jarosite precipitation: reactions at 150° and the mechanism of arsenic precipitation: Can. Metall. Quart., v. 26, no. 2, p. 103–115.

Eary, L. E., 1999, Geochemical and equilibrium trends in mine pit lakes: Appl. Geochem., v. 14, p. 963–987.

Eggleston, C. M., Ehrhardt. J.-J., and Slumm, W., 1996, Surface structural controls on pyrite oxidation kinetics: An XPS-UPS, STM, and modeling study: Amer. Mineral., v. 81, p. 1036–1056.

Eisler, R., 1994, A review of arsenic hazards to plants and animals with emphasis on fishery and wildlife resources, *in* Nriagu, J. O., ed., Arsenic and the environment Part II: Human health and ecosystem effects: New York, John Wiley & Sons, Inc., p. 185–259.

Evangelou, V. P., Seta, A. K., and Holt, A., 1998, Potential role of bicarbonate during pyrite oxidation: Environ. Sci. Technol., v. 32, p. 2084–2091.

Evangelou, V. P., and Zhang, Y. L., 1995, A review: Pyrite oxidation mechanisms and acid mine drainage prevention: Crit. Rev. Environ. Sci. Technol., v. 25, p. 141–199.

Ferguson, H. G., 1914, Lode deposits of the Alleghany district, California. U.S. Geol. Surv. Bull. 580.

Ferguson, J. F., and Gavis, J., 1972, A review of the arsenic cycle in natural waters: Water Res., v. 6, p. 1259–1274.

Fleet, M. E., Chryssoulis, S. L., MacLean, P. J., Davidson, R., and Weisener, C. G., 1993, Arsenian pyrite from gold deposits: Gold and arsenic distribution investigated by SIMS and EMP, and color staining and surface oxidation by XPS and LIMS: Can. Mineral., v. 31, p. 1–17.

Foster, A. L., Brown, G. E., Jr., Tingle, T. N., and Parks G. A., 1998, Quantitative arsenic speciation in mine tailings using x-ray absorption spectroscopy: Amer. Mineral., v. 83, p. 553–568.

Frost, R. R., and Griffin, R. A., 1977, Effect of pH on adsorption of arsenic and selenium from landfill leachate by clay minerals: Soil Sci. Soc. Amer. Jour., v. 41, p. 53–57.

Goudey, H., 1947, Scorodite near Jamestown, California: Mineral Notes and News Bull., v. 114, p. 12.

Hem, J. D. 1977, Reactions of metal ions at surfaces of hydrous iron oxide: Geochim. et Cosmochim. Acta, v. 41, p. 527–538.

Huggins, F. E., Srikantapura, S., Parekh, B. K., Blanchard, L., and Robertson, J. D., 1997, XANES spectroscopic characterization of selected elements in deep-cleaned fractions of Kentucky No. 9 coal: Energy Fuels, v. 11, p. 691–701.

Hunerlach, M. P., and Alpers, C. N., 1994, Analysis of fracture orientations in surface outcrops and boreholes in the vicinity of an acidic ground-water plume at Penn Mine, Calaveras County, California [abs.]: Amer. Geophys. Union Abs. Prog., v. 75, no. 44, p. 243.

Jambor, J. L., 1994, Mineralogy of sulfide-rich tailings and their oxidation products, *in* Jambor, J. L., and Blowes, D. W., eds., Environmental geochemistry of sulfide mine-wastes, v. 22: Waterloo, Ont., Mineral. Assoc. Canada.

Jaynes, D. B., Rogowski, A. S., and Pionke, H. B., 1984, Acid mine drainage from reclaimed coal strip mines: I. Model description: Water Resources Res., v. 20, p. 233.

Kistler, R. W., Dodge, R. C. W., and Silberman, M. L., 1983, Isotopic studies of mariposite-bearing rocks from the south-central Mother Lode, California: Calif. Geol., Sept. 1983, p. 201–203.

Knopf, A., 1929, The Mother Lode system of California: U. S. Geol. Surv. Prof. Pap. 157.

Kuhl, T. O., and Lechner, M. J., 1990, Geologic summary of the Royal Mountain King Mine, *in* Seedorff, E., ed., Geology and ore deposits of the Sierra Nevada and foothills; Mary Harrison Prospect, Royal Mountain King mine, Lincoln mine, Spanish mine, v. 11: Reno, NV, Geol. Soc. Nevada, p. 96–100.

Kuhn, A., and Sigg, L., 1993, Arsenic cycling in eutrophic Lake Greifen, Switzerland: Influence of seasonal redox processes: Limnol. Oceanog., v. 38, p. 1052–1059.

Landefeld, L. A., and Snow, G. G., 1991, Yosemite and the Mother Lode gold belt: Geology, tectonics, and the evolution of hydrothermal fluids in the Sierra Nevada of California: Guidebook—Pacific Section, Amer. Assoc. Petrol. Geol. 68.

Lindgren, W., 1896, The gold quartz veins of Nevada City and Grass Valley districts, California: U. S. Geol. Surv. Ann. Report 17, part 2.

Mandl, M., and Vyskovsky, M., 1994, Kinetics of arsenic(III) oxidation by iron(III) catalysed by pyrite in

the presence of *Thiobacillus ferrooxidans*: Biotechnol. Lett., v. 16, p. 1199–1204.

Manning, B. A., Fendorf, S. E., and Goldberg, S., 1998, Surface structures and stability of arsenic(III) on goethite: Spectroscopic evidence for inner-sphere complexes: Environ. Sci. Technol., v. 32, p. 2383–2388.

Manning, B. A., and Goldberg, S., 1996, Modeling competitive adsorption of arsenate with phosphate and molybdate on oxide minerals: Soil Sci. Soc. Amer. Jour., v. 60, p. 121–131.

McKibben, M. A., and Barnes, H. L., 1986, Oxidation of pyrite in low temperature acidic solutions: Rate laws and surface textures: Geochim. et Cosmochim. Acta, v. 50, p. 1509–1520.

Moller, P., and Kersten, G., 1994, Electrochemical accumulation of visible gold on pyrite and arsenopyrite surfaces: Mineralium Deposita, v. 29, p. 404–413.

Moses, C. O., and Herman, J. S., 1991, Pyrite oxidation at circumneutral pH: Geochim. et Cosmochim. Acta, v. 55, p. 471–482.

Moses, C. O., Nordstrom, D. K., Herman, J. S., and Mills, A. L., 1987, Aqueous pyrite oxidation by dissolved oxygen and by ferric iron: Geochim. et Cosmochim. Acta, v. 51, p. 1561–1571.

Nelson, G. M., and Leicht, W., 1994, Native gold from the Jamestown mine, Tuolumne County, California: Mineral. Rec., v. 25, p. 7–14.

Nesbitt, H. W., Muir, I. J., and Pratt, A. R., 1995, Oxidation of arsenopyrite by air and air-saturated, distilled water, and implications for mechanism of oxidation: Geochim. et Cosmochim. Acta, v. 59, p. 1773–1786.

Nicholson, R. V., Gillham, R. W., and Reardon, E. J., 1988, Pyrite oxidation in carbonate-buffered solution; 1, Experimental kinetics: Geochim. et Cosmochim. Acta, v. 54, p. 395–402.

_____, 1990, Pyrite oxidation in carbonate-buffered solution; 2. Rate control by oxide coatings: Geochim. et Cosmochim. Acta, v. 54, p. 395–402.

Parsons, A. B., 1920, The mine and mill of the Belmont Shawmut Mining Co.: Min. and Sci. Press, v. 121, p. 619–624.

Parsons, M. B., Bird, D. K., Einaudi, M. T., and Alpers, C. N., in press, Geochemical and mineralogical controls on trace element release from base-metal smelter slags: Appl. Geochem.

Peterson, M. L., and Carpenter, R., 1986, Arsenic distributions in porewaters and sediments of Puget Sound, Lake Washington, the Washington coast, and Saanich Inlet, B. C.: Geochim. et Cosmochim. Acta, v. 50, p. 353–369.

Plumlee, G. S., Smith, K. S., and Ficklin, W. H., 1994, Geoenvironmental models of mineral deposits, and geology-based mineral-environmental assessments of public lands: U.S. Geol. Surv. Open File Report 94–203.

Pokrovski, G., Gout, R., Schott, J., Zotov, A., and Harrichoury, J. C., 1996, Thermodynamic properties and stoichiometry of As(III) hydroxide complexes at hydrothermal conditions: Geochim. et Cosmochim. Acta, v. 601, p. 737–749.

Pontius, F. W., 1995, Uncertainties drive arsenic rule delay: Jour. Amer. Water Works Assoc., v. 87, no. 4, p. 12, 150.

Pouchou, J. L., and Pichoir, F., 1985, "PAP" $\phi\rho Z$ procedure for improved quantitative microanalysis, *in* Armstrong, J. T., ed., Microbeam analysis: San Francisco, San Francisco Press, Inc., p. 104–106.

Sanches Montero, I., Brimhall, G., Alpers, C., and Swayze, G. A., 1999, Use of UV/VIS/IR spectroscopy to characterize mine waste dumps in Penn Mine, Calaveras County, California [abs.]: Geol. Soc. Amer. Abs. Prog., v. 31, no. 6, p. A91.

Sanders, J. G., Riedel, G. F., and Osman, R. W., 1994, Arsenic cycling and its impact in estuarine and coastal marine ecosystems, *in* Nriagu, J. O., ed., Arsenic in the environment. Part I: Cycling and characterization: New York, John Wiley & Sons, Inc., p. 289–308.

Savage, K. S., Tingle, T. N., O'Day, P. A., Waychunas, G. A., and Bird, D. K., 2000, Arsenic speciation in pyrite and secondary weathering phases, Mother Lode Gold District, Tuolumne County, California: Appl. Geochem., in press.

Schweickert, R. A., Bogen, N. L., and Merguerian, C., 1988, Deformational and metamorphic history of Paleozoic and Mesozoic basement terranes in the western Sierra Nevada metamorphic belt, *in* Ernst, W. G., ed., Rubey Colloquium on Metamorphism and Crustal Evolution of the Western United States, v. 7, Englewood Cliffs, NJ: Prentice-Hall, p. 789–822.

Schweickert, R. A., Hanson, R. E., and Girty, G. H., 1999, Accretionary tectonics of the Western Sierra Nevada metamorphic belt, *in* Wagner, D. G., and Graham, S. A., eds., Geologic field trips in northern California: Centennial meeting of the Cordilleran Section, Geol. Soc. Amer., v. 119: Sacramento, CA, Calif. Dept. Conservat., Div. Mines and Geol., p. 33–79.

Seyler, P., and Martin, J.-M., 1989, Biogeochemical processes affecting arsenic species distribution in a permanently stratified lake: Environ. Sci. Technol., v. 23, p. 1258–1263.

Singer, P. C., and Stumm, W., 1970, Acidic mine drainage: The rate-determining step: Science, v. 167, p. 1121–1123.

Slotton, D. G., and Reuter, J. E., 1995, Heavy metals in intact and resuspended sediments of a California Reservoir, with emphasis on potential bioavailability of copper and zinc: Marine Freshwater Res., v. 46, p. 257–265.

Smith, K. S., Ficklin, W. H., Plumlee, G. S., and Meier, A. L., 1992, Metal and arsenic partitioning between water and suspended sediment at mine-drainage sites in diverse geologic settings, *in* Water-Rock Interact., Proc. Int. Symp., 7th, p. 443–447.

Stolz, J. F., and Oremland, R. S., 1999, Bacterial respiration of arsenic and selenium: Fems Microbiol. Rev., v. 23, p. 615–627.

Stumm, W., and Morgan, J. J., 1996, Aquatic chemistry: New York, John Wiley and Sons.

Taylor, S. R., and McLennan, S. M., 1985, The continental crust: Its composition and evolution: Oxford, UK: Blackwell Scientific Publ.

Thanabalasingam, P., and Pickering, W. F., 1986, Effect of pH on interaction between As(III) or As(V) and manganese(IV) oxide: Water, Air, and Soil Pollution, v. 29, p. 205–216.

Tingle, T. N., Waychunas, G. A., Bird, D. K., and O'Day, P. A., 1996, X-ray absorption spectroscopy (EXAFS) of arsenic solical solution in pyrite, Clio mine, Mother Lode Gold District, Tuolumne County [abs.]: Geol. Soc. Amer. Abs. Prog., v. 28, no, 7, p. 518.

Wagner, J. R., 1970, Gold mines of California: Berkeley, CA: Univ. Calif. Press.

Waychunas, G. A., Davis, J. A., and Fuller, C. C., 1995, Geometry of sorbed arsenate on ferrihydrite and crystalline FeOOH; re-evaluation of EXAFS results and topological factors in predicting sorbate geometry, and evidence for monodentate complexes: Geochim. et Cosmochim. Acta, v. 59, p. 3655–3661.

Waychunas, G. A., Rea, B. A., Fuller, C. C., and Davis, J. A., 1993, Surface chemistry of ferrihydrite: Part 1. EXAFS studies of the geometry of coprecipitated and adsorbed arsenic: Geochim. et Cosmochim. Acta, v. 57, p. 2251–2269.

Weir, R. H. J., and Kerrick, D. M., 1987, Mineralogic, fluid inclusion, and stable isotope studies of several gold mines in the Mother Lode, Tuolumne and Mariposa counties, California: Econ. Geol., v. 82, p. 328–344.

Williamson, M. A., and Rimstidt, J. D., 1994, The kinetics and electrochemical rate-determining step of aqueous pyrite oxidation: Geochim. et Cosmochim. Acta, v. 58, p. 5443–5454.

Wilkie, J. A., and Hering, J. G., 1996, Absorption of arsenic onto hydrous ferric oxide: Effects of adsorbate/adsorbent ratios and co-occurring solutes: Colloids and Surfaces A, v. 107, p. 97–110.

Ziarkowski, D. V., 1999, Human encroachment on areas of historic mining: Mesa de Oro subdivision/Central Eureka Mine case study: Geol. Soc. Amer. Abs. Prog., v. 31, no. 6, p. A113.